http://dx.doi.org/10.1097/mm9.0000000000000031

MedMat

Review

OPEN

Functional advancements in intravascular catheters: materials, sensors, actuators, and robot integration

Chuqiao Lyu[a], Qinghao Xu[a], Shoujie Li[a], Eric J. Chen[a], Wenxuan Zhu[a], Hongliang Ren[b], Wenbo Ding[a,*]

Abstract

The intravascular catheter is undergoing a fundamental transformation from a passive conduit to an intelligent, multifunctional medical device. Recent advancements in catheter materials include biocompatible polymers, lubricious coatings, and variable stiffness architectures, which have significantly enhanced mechanical performance and compatibility within the vascular environment. In parallel, catheter sensing technologies have enabled real-time physiological and mechanical feedback, supporting precise diagnosis and targeted intervention, while actuated catheters with advanced motion control mechanisms have further improved maneuverability in complex vascular pathways. These advancements are further augmented by robot-assisted catheterization platforms, which enhance navigation accuracy, reduce radiation exposure, and facilitate complex procedures through diverse actuation and teleoperation. Previous research on intravascular catheters has largely focused on individual technical aspects in isolation, lacking a comprehensive perspective on material innovations, sensing capabilities, actuated mechanisms, and robotic systems. Therefore, this review systematically examines current intravascular catheter technologies, focusing on the integration of advanced catheter materials, embedded sensing capabilities, actuated catheter designs, and robotic systems. These innovations represent a significant advancement toward safer, more effective, and autonomous endovascular therapies.

Keywords: Actuated catheter, Catheter material, Catheter sensor, Intravascular catheter, Robot-assisted catheterization

1. Introduction

In recent years, cardiovascular and cerebrovascular diseases have emerged as leading threats to global health[1,2]. Intravascular catheters are central to a range of endovascular interventions, including percutaneous coronary intervention (PCI), catheter ablation, mechanical thrombectomy, and targeted embolization[3]. Owing to their flexibility, steerability, and anatomical compatibility, intravascular catheters can reach deep-seated lesions through minimally invasive access[4,5]. Despite their widespread use in modern interventional procedures, conventional intravascular catheters are passive tools, lacking capabilities such as real-time sensing or active navigation[6]. Their roles are typically confined to single-purpose tasks like fluid delivery, energy ablation, or stent placement. As a result, procedural success depends heavily on operator expertise, and complications such as vessel injury, inaccurate targeting, or incomplete treatment continue to pose significant clinical risks[7].

[a]Shenzhen International Graduate School, Tsinghua University, Shenzhen, China, [b]Department of Electronic Engineering, The Chinese University of Hong Kong, Hong Kong.

*Corresponding author: Address: Wenbo Ding, Shenzhen International Graduate School, Tsinghua University, Shenzhen, China. Tel: 86-15801390093; E-mail address: ding.wenbo@sz.tsinghua.edu.cn (W. Ding).

Chuqiao Lyu and Qinghao Xu contributed equally to this work.

MedMat (2025) 2:4

Received: 31 July 2025; Accepted 6 November 2025

Published online 13 November 2025

Functionalized intravascular catheters (Figure 1), which integrate sensing, actuation, and intelligent control into flexible intravascular devices, are reshaping the landscape of minimally invasive therapy[18–21]. To facilitate catheter insertion and navigation through tortuous vasculature, lubricating materials (Figure 1A)[8] have been introduced to significantly reduce friction against vessel walls, thereby enhancing procedural safety. Intravascular sensors (Figure 1B)[9], such as those measuring pressure, flow, and temperature, allow for continuous physiological monitoring within the vessel. At the systems level, teleoperation robots (Figure 1C)[10] isolate the operator from radiation exposure while providing intuitive control over the catheter. Navigation robots (Figure 1D)[11], incorporating image-guided or electromagnetic tracking, improve the accuracy and automation of catheter positioning. On the therapeutic front, actuated catheters equipped with mechanical thrombectomy or ablation devices (Figure 1E)[12] enable active intervention at the treatment site, particularly in the management of ischemic stroke or pulmonary embolism.

In addition, steerable catheters (Figure 1F)[13], actuated through tendon-driven or hydraulic mechanisms, offer real-time tip control for complex vascular navigation. Microelectromechanical systems (MEMS) sensors (Figure 1G)[14] further miniaturize and integrate high-resolution sensing functions, supporting precise catheter vessel interaction through enhanced force and motion detection. Variable stiffness materials (Figure 1H)[15], developed through composite structures or integrated shape memory alloys, allow catheters to adaptively transition between rigid and flexible segments, improving maneuverability and anatomical conformity. Magnetic robotic systems (Figure 1I)[16] enable remote, contactless guidance of magnetically responsive catheters, expanding the potential for

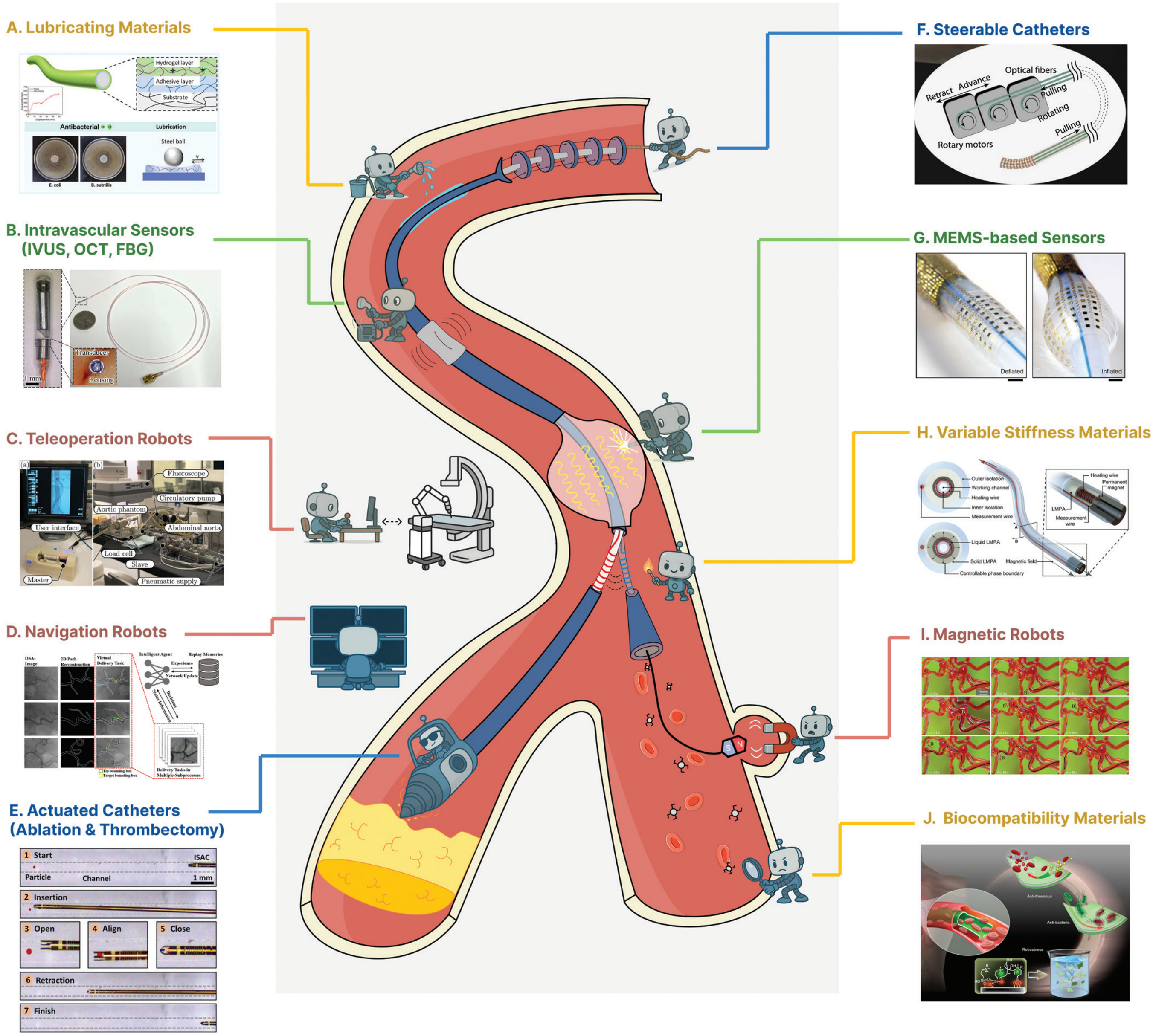

Figure 1. Functionalized intravascular catheter systems. Each behavior of the small robot in the figure symbolizes 1 function of the interventional catheter system. (A, H, J) The yellow lines indicate catheter material enhancements. (B, G) The green denotes sensor integration. (E, F) The blue lines represent actuated catheters. (C, D, I) The red lines indicate robotic integration. (A) Lubricious materials reduce friction between the catheter and vessel wall, minimizing surgical risk. Reproduced with permission from Zhang et al.[8] Copyright 2025, American Chemical Society. (B) Intravascular sensors (including IVUS, OCT, and FBG) enable data acquisition in confined vascular environments. Reproduced with permission from Yang et al.[9] Copyright 2025, IEEE. (C) Teleoperation robots utilize master-slave control to reduce operator radiation exposure. Reproduced with permission from Kundrat et al.[10] Copyright 2025, IEEE. (D) Navigation robots employ imaging-based positioning to achieve automated and intelligent catheter manipulation. Reproduced with permission from Mei et al.[11]. Copyright 2025, IEEE. (E) Actuated catheters deploy mechanical tools at the tip to perform tasks such as thrombectomy and ablation. Reproduced with permission from Rivkin et al.[12] Copyright 2021, The American Association for the Advancement of Science. (F) Active catheters use tendon-driven or hydraulic mechanisms to steer the catheter tip. Reproduced with permission from Zhou et al.[13] Copyright 2024, The American Association for the Advancement of Science. (G) Incorporate MEMS to enhance catheter functionality. Reproduced with permission from Han et al.[14] Copyright 2020, Springer Nature. (H) Variable stiffness materials adapt their rigidity to maintain catheter shape within complex vasculature. Reproduced with permission from Lussi et al.[15] Copyright 2021, Wiley-VCH GmbH. (I) Magnetic robots enable navigation of magnetically responsive catheters or microrobots via external magnetic fields. Reproduced with permission from Kim et al.[16] Copyright 2019, The American Association for the Advancement of Science. (J) Biocompatible materials, including biodegradable and antimicrobial coatings, help reduce postoperative complications. Reproduced with permission from Liu et al.[17]. Copyright 2024, Springer Nature.

fully autonomous interventions. Biocompatible materials (Figure 1J)[17] form the basis for safe and sustained vascular interaction, minimizing immune responses and reducing the risk of thrombosis during prolonged interventions. Collectively, these innovations converge to create functionalized intravascular catheter systems integrating material science, sensing, actuation, and robotics. They lay the groundwork for clinically deployable, endovascular systems with enhanced autonomy and therapeutic precision. In this review, actuated catheters are defined as systems that integrate a therapeutic module mounted on the tip. Steerable catheters refer to manually controlled devices that achieve distal motion through mechanical means such as pull-wires, hydraulic channels, or tendon drives. Robotic catheters describe systems operated or assisted by external robotic platforms or magnetic navigation, which integrate imaging and sensor feedback to enable semiautonomous or fully automated operation.

This review opens with an overview of major vascular interventional procedures, outlining the clinical scenarios in which catheter technologies are applied. This context highlights the functional requirements placed on intravascular devices across a range of therapeutic applications. The discussion then turns to recent developments in catheter materials, including biocompatible substrates, low-friction surface treatments, and variable stiffness structures designed to improve maneuverability and safety. Integrated sensing technologies are examined next, focusing on intravascular ultrasound (IVUS), optical coherence tomography (OCT), fiber Bragg grating (FBG) sensors, and MEMS sensors that provide real-time physiological and mechanical feedback. The review also explores tip-mounted actuated catheters, such as those for ablation, thrombectomy, and tissue manipulation. Robotic integration is addressed in detail, including steerable catheter designs, image-guided navigation, magnetic control systems, and teleoperation platforms. Taken together, these advancements serve as enabling technologies for intelligent intravascular interventions. The review concludes by discussing key technical challenges and future directions in the development of fully integrated, intelligent intravascular robotic systems.

2. Interventional catheterization

Interventional catheterization encompasses a broad spectrum of minimally invasive procedures used to diagnose and treat vascular pathologies[22]. Performed under real-time imaging guidance, these interventions enable access to deep vascular structures via percutaneous routes. Catheters vary in size, geometry, and functionality depending on the clinical application, but all aim to minimize tissue injury, improve accuracy, and support faster recovery. Common procedures include:

PCI[23]. A primary treatment for coronary artery disease involving balloon dilation and stent placement to reopen narrowed coronary arteries.

Electrophysiological ablation[24]. Thermal or electrical ablation delivered via intracardiac catheters to eliminate arrhythmogenic foci in the treatment of atrial fibrillation and other rhythm disorders.

Mechanical thrombectomy[25]. Used in acute stroke and pulmonary embolism, these catheters retrieve or fragment thrombi to restore perfusion.

Endovascular embolization[26]. Delivery of embolic materials to occlude abnormal or hemorrhagic vessels, often applied in aneurysm repair or arteriovenous malformations.

Atherectomy and plaque modification[27]. Debulking of calcified or fibrotic plaques using rotational, orbital, or directional drilling systems to facilitate revascularization.

Endovascular aortic repair[28]. Endovascular placement of stent grafts to isolate and reinforce aneurysmal segments of the aorta or peripheral vessels.

Despite their diversity, these procedures remain highly dependent on operator experience and continuous imaging, as traditional catheters largely function as passive instruments[6]. This reliance introduces limitations in precision, consistency, and responsiveness, particularly in complex or prolonged interventions.

To address these challenges, the functionalized intravascular catheters (Figure 2) are emerging, aiming to enhance materials, sensors, actuators, and robotic integration. These innovations are profoundly reshaping the field of endovascular intervention. Their development underscores the critical need for alignment between engineering solutions, procedural workflows, and clinical objectives. Ultimately, such integration ensures optimal therapeutic outcomes across a wide range of vascular pathologies. Furthermore, these advancements pave the way for data-driven, semiautonomous interventional platforms with embedded intelligence, promoting greater safety, efficiency, and procedural reproducibility.

3. Catheter materials

The performance of intravascular catheters is closely tied to the properties of the materials from which they are constructed. In addition to providing structural integrity and mechanical flexibility, these materials must meet strict biological standards due to prolonged contact with blood and vascular tissues[29]. As procedural complexity increases, catheter materials must offer more than just biocompatibility. Advanced features such as low-friction surfaces, adjustable stiffness, and compatibility with embedded electronics have become essential[30]. This section summarizes recent progress in catheter materials, with particular attention to innovations in biocompatible substrates, lubricious coatings, and variable-stiffness architectures that enable adaptive performance within the vasculature.

3.1 Biocompatible materials

Biocompatibility (Figure 3) is a core requirement for catheter materials given their sustained exposure to blood and vessel walls. Ideal materials should minimize immune activation, resist thrombosis, and maintain long-term mechanical and chemical stability in physiological environments. Commonly used polymers such as polyurethane (PU), silicone, and polyethylene terephthalate are favored for their flexibility and baseline hemocompatibility[35]. Fluorinated polymers like polytetrafluoroethylene (PTFE) are also widely studied for their low surface energy and reduced protein adsorption, which limit the thrombus formation. Recent research efforts have focused on enhancing antifouling properties and biological inertness through advanced surface modifications and functional coatings[36].

To address challenges related to thrombosis and infection, functional surface coatings have gained increasing attention. Liu et al. (Figure 3A)[17] developed a heparin network coating that significantly suppressed thrombus adhesion in vitro while achieving high antibacterial efficiency against both *Staphylococcus aureus* and *Escherichia coli*. Zhang et al. (Figure 3B)[31] also introduced hydrophobic domains into heparin films via ethyl lauroyl arginate (ELA), enhancing coating stability and antibacterial performance. The resulting ELA heparin complex sustained heparin release for 21 days and reduced bacterial colonization by more than 99%, thereby overcoming the burst-release limitation associated with unmodified hydrophilic coatings. More recently, bioinspired dynamic materials have emerged. Wang et al. (Figure 3C)[32,37] fabricated magnetically responsive hydrogel fibers from autologous blood and magnetic nanoparticles for intracranial use; the fibers matched brain tissue stiffness (~100 kPa) and enabled on-demand drug release under a magnetic field while maintaining integrity in confined channels. Park et al. (Figure 3D)[33] developed a porous carboxymethyl chitosan (p-CMC)-coated catheter that reduced *E. coli* and platelet adhesion by over 90% while enhancing

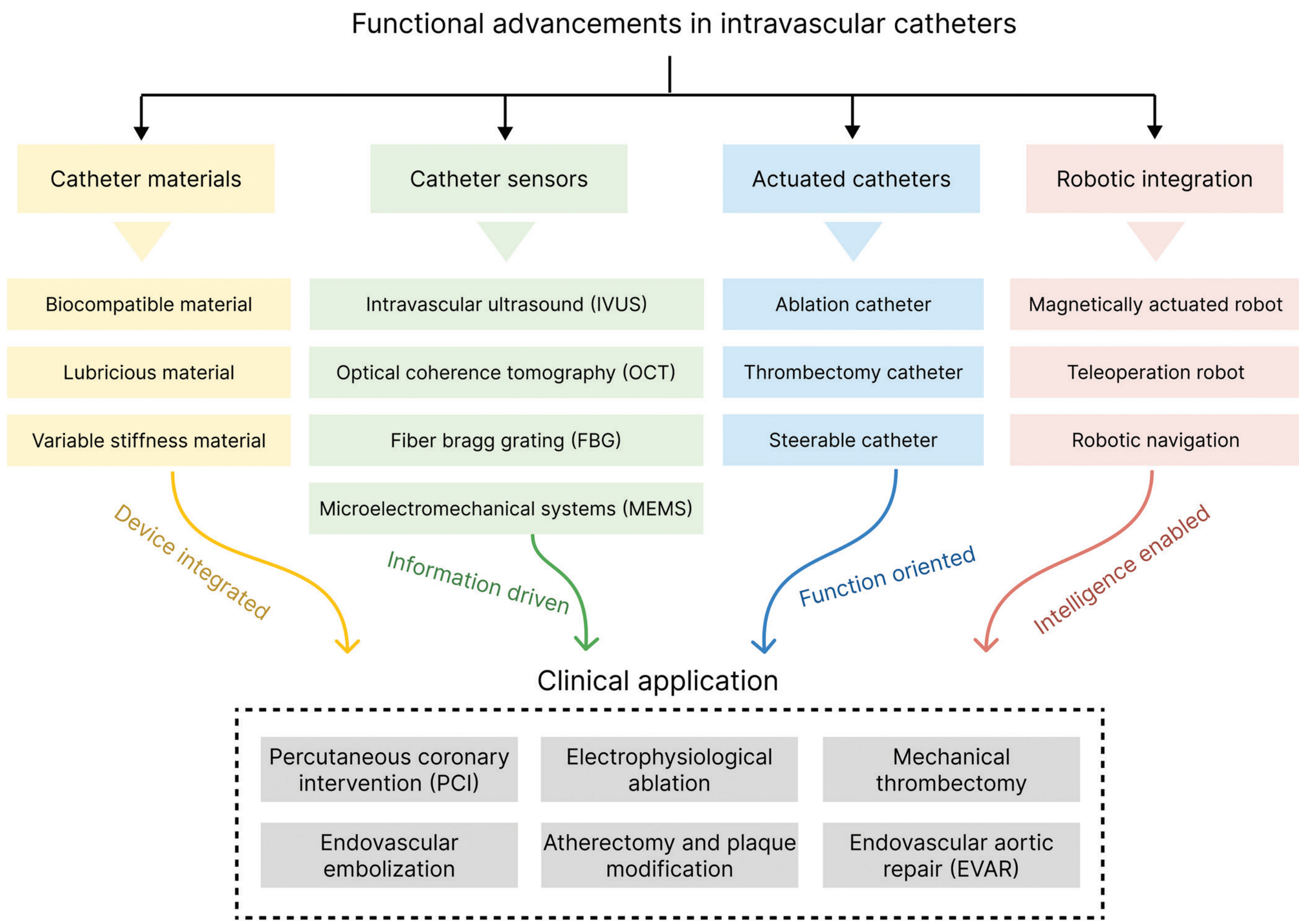

Figure 2. Schematic classification of functionalized intravascular catheters.

trackability and durability. Zhang et al. (Figure 3E)[34] reported a PTFE coating modified with imipenem/cilastatin sodium via dendritic mesoporous silica nanoparticles (IC@dMSNs), achieving >99.9% antibacterial efficiency.

Overall, balancing mechanical robustness, controlled degradability, and long-term biocompatibility of the catheter remains challenging. Specifically, we note that intravascular catheter systems must comply with international sterilization and regulatory standards to ensure clinical translation. Common sterilization methods include ethylene oxide (ISO 11135:2014[38]) and steam sterilization (ISO 17665-1:2024[39]). Adherence to these standards ensures material safety, sterilization stability, and provides a clear pathway toward clinical application.

3.2 Lubricious materials

Lubricity (Figure 4) is a key requirement for intravascular catheters, enabling smooth navigation through complex vascular anatomy while minimizing endothelial damage. To address this, various surface modification strategies have been explored to reduce interfacial friction and improve clinical maneuverability. Among these, hydrophilic coatings have attracted particular interest due to their ability to form stable hydration layers that significantly lower the coefficient of friction (COF)[8].

For example, Lai et al. (Figure 4A)[40] developed a polyvinylpyrrolidone–polyethylene glycol (PVP–PEG) copolymer coating on thermoplastic polyurethane (TPU) substrates, which achieved long-lasting lubricity under physiological flow, maintaining low COF and excellent mechanical integrity after 60 cycles of wet friction testing. Similarly, Zhang et al. (Figure 4B)[8] designed a waterborne polyurethane (WPU) stabilized hydrogel coating with a low COF of 0.0357 under 1 Hz reciprocating motion, along with an interfacial bonding strength up to 536 N/m, indicating both robust adhesion and durable lubrication. The coating also demonstrated antimicrobial efficacy with inhibition zones of 4.2 mm (*Bacillus subtilis*) and 1.9 mm (*E. coli*). Beyond traditional hydrogel approaches, liquid-infused and bioinspired coatings have demonstrated unique capabilities. Wang et al. (Figure 4C)[41] developed a liquid-fibrous catheter with spatially controlled drug release and adaptive lubrication. The COF varied depending on drug properties and pore size, highlighting the crucial role of matrix liquid interactions. Park et al.[33] introduced a p-CMC coating via selective PEG leaching. The p-CMC exhibited superhydrophilicity and a significant reduction in COF while maintaining performance over 60 minutes of continuous friction. The coating also reduced bacterial and platelet adhesion, thereby enhancing biocompatibility.

Although hydrophobic coatings generally lack hydration lubrication, certain designs achieve reduced adhesion via low surface energy or physical surface structuring. Armugam et al. (Figure 4D)[42] synthesized a PDMS catheter coating exhibiting intrinsic hydrophobicity and notable broad-spectrum antimicrobial activity, suitable for long-term implantation. In another approach, Zhang et al. (Figure 4E)[34] utilized a PTFE coating loaded with IC@dMSNs. This construction demonstrated a 6.4% increase in antibacterial efficacy against *E. coli* (from

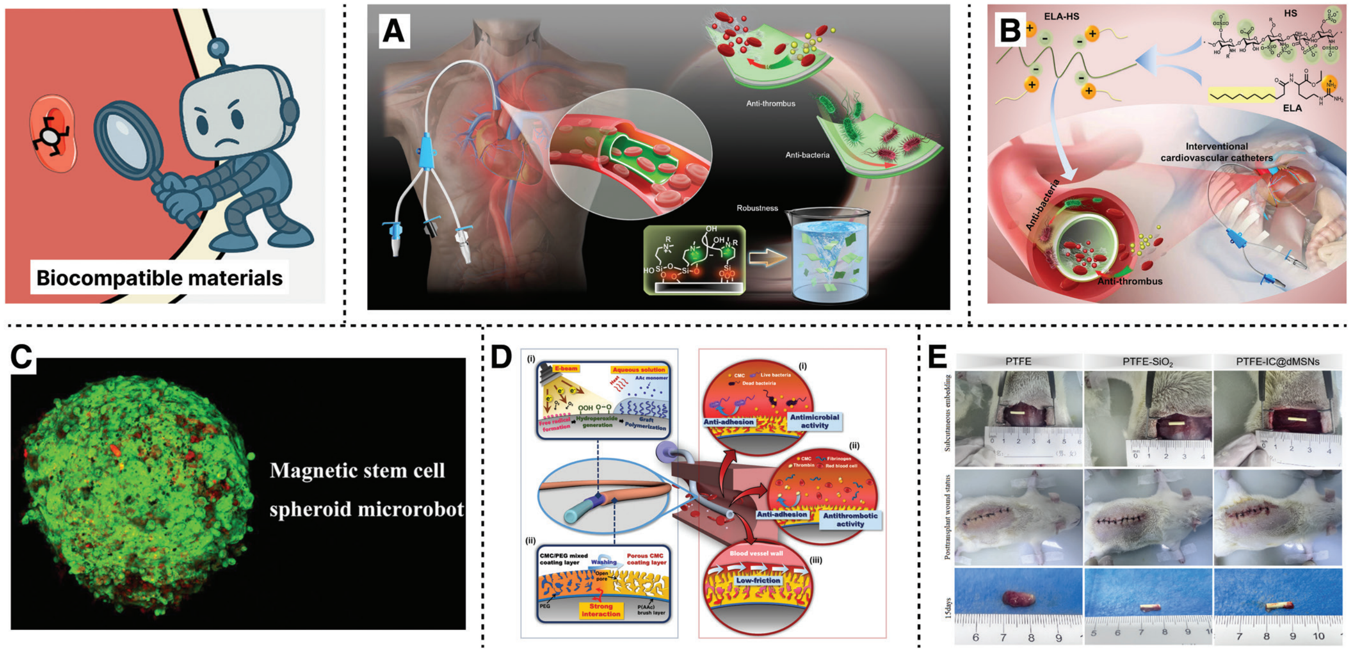

Figure 3. Biocompatible materials. (A) Heparin network coating for thrombosis and infection. Reproduced with permission from Liu et al.[17] Copyright 2024, Springer Nature. (B) Hydrophobic modified heparin coating. Reproduced with permission from Zhang et al.[31] Copyright 2025, Elsevier. (C) Magnetic stem cell. Reproduced with permission from Wang et al.[32] Copyright 2021, The American Association for the Advancement of Science. (D) Porous CMC multifunctional coating. Reproduced with permission from Park et al.[33] Copyright 2022, Elsevier. (E) Superhydrophobic PTFE antibacterial coating. Reproduced with permission from Zhang et al.[34] Copyright 2023, Elsevier.

50.8% to 56.9%) and a 5.8% increase against *S. aureus* (from 83.5% to 89.3%), along with sustained anticoagulant function and hydrophobicity (water contact angle >150 °). Integrating multifunctional coatings has emerged as a frontier. Lim et al.[43] constructed a polydopamine peptide surface with combined antimicrobial, antithrombotic, and lubricating functions using a 1-step immobilization strategy.

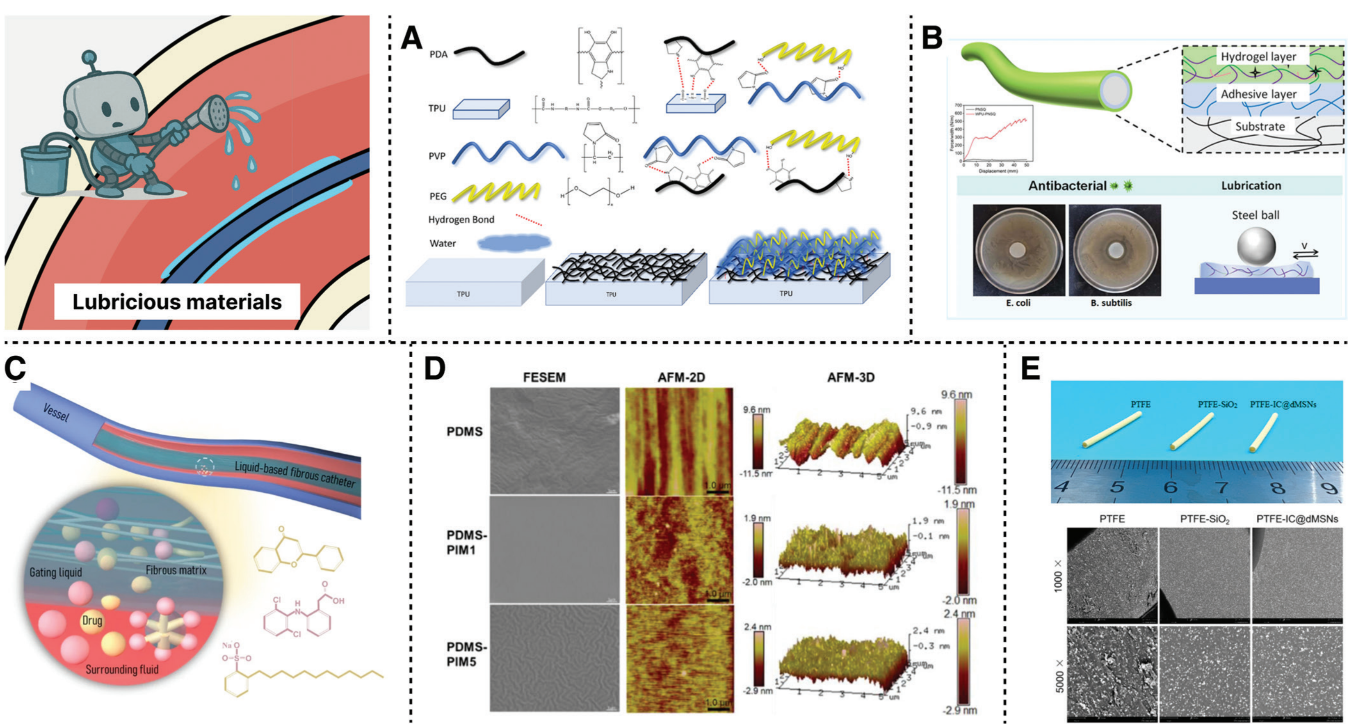

Figure 4. Lubricious materials. (A) PVP–PEG copolymer coating on TPU. Reproduced with permission from Lai et al.[40] Copyright 2024, Elsevier. (B) WPU stabilized hydrogel with strong adhesion. Reproduced with permission from Zhang et al.[8] Copyright 2025, American Chemical Society. (C) Liquid-infused catheter with drug release. Reproduced with permission from Wang et al.[41] Copyright 2022, Springer Nature. (D) PDMS antimicrobial hydrophobic coating. Reproduced with permission from Armugam et al.[42] Copyright 2021, Springer Nature. (E) PTFE-IC@dMSNs. Reproduced with permission from Zhang et al.[34] Copyright 2023, Elsevier.

Although significant progress has been made, challenges such as coating delamination, limited durability under dynamic blood flow, and difficulties integrating embedded functionalities still persist. To overcome these issues, continued efforts in developing bioinspired, multifunctional, and stable lubricating coatings will be instrumental in advancing intravascular catheter systems.

3.3 Variable stiffness materials

Variable stiffness (Figure 5) is a critical functional requirement for intravascular catheters, balancing rigidity for navigation with flexibility for safe traversal of tortuous vasculature. Traditional designs often incorporate passive stiffness gradients, but these lack intraoperative adaptability. Recent advancements focus on active stiffness modulation through phase change materials, smart polymers, and engineered architectures that respond to thermal, electrical, or magnetic stimuli.

Thermally responsive shape memory polymers (SMPs), particularly PU or thermoset variants, offer large modulus changes when transitioning across their glass transition temperature. For instance, Mattmann et al. (Figure 5A)[44] developed a thermoset SMP catheter with heating times of ~7 s and cooling below 15 s. The device maintained biocompatibility and stiffness reversibility without the need for encapsulation, illustrating the feasibility of rapid intraoperative stiffness tuning. Piskarev et al. (Figure 5B)[45] introduced a conductive SMP variable stiffness thread that combines stiffness modulation with integrated heating and sensing functions. Their device achieved a stiffness change factor of 21 and enabled selective segmental bending under a 20 mT magnetic field in a 2.0 mm diameter catheter. To improve response time and scalability, Piskarev et al.[49] also developed a fast-response SMP catheter with integrated water cooling, achieving a 26-fold faster stiffening response (from 115 s to 4.4 s) and a 66-fold change in modulus within a 2.3 mm-diameter profile. This work highlights the importance of integrating efficient thermal management strategies for clinical applicability. Choi et al.[50] extended this paradigm with thermally drawn SMP fibers (SMPFs), enabling continuous fabrication of long-length catheters with embedded wires and lumens for actuation, sensing, and fluid transport. Their SMPF catheter exhibited a 31-fold change in stiffness within 8.4 s and operated safely within the 20–37 °C temperature window. Phantom studies confirmed stable navigation and shape locking in tortuous vasculature.

Low-melting-point alloys (LMPAs) offer an extreme stiffness ratio (>400 times) and have been used in magnetic-steering catheters. Mao et al. (Figure 5C)[46] demonstrated a 3–4 mm diameter catheter incorporating alternating "Guider" and "Follower" segments, each composed of LMPAs, achieving apical elongation and following the leader (FTL) behavior under magnetic actuation. Their system responded within 5–10 s for softening and ~15 s for restiffening in water environments, maintaining safe surface temperatures under 50 °C. Other variable stiffness mechanisms include jamming systems (granular, layer, or fiber), which exhibit <1 s response times but are difficult to miniaturize below 3 mm diameter due to the need for air channels or particles. While suitable for larger endoscopic instruments, their bulk limits cardiac applications. In contrast, fiber-jamming catheters, such as those by Sun et al. (Figure 5D)[48], achieve rapid stiffness modulation within sub-2.5 mm diameters suitable for cardiovascular use. Fabrication approaches also influence design feasibility. Thermal drawing, as demonstrated by Abdelaziz et al. (Figure 5E)[48], allows rapid prototyping of multilumen, tendon-driven, or actively tracked catheters with programmable mechanical and imaging properties, showing comparable performance to commercial systems in preclinical trials. These approaches support broader integration with MR guidance or robotic control.

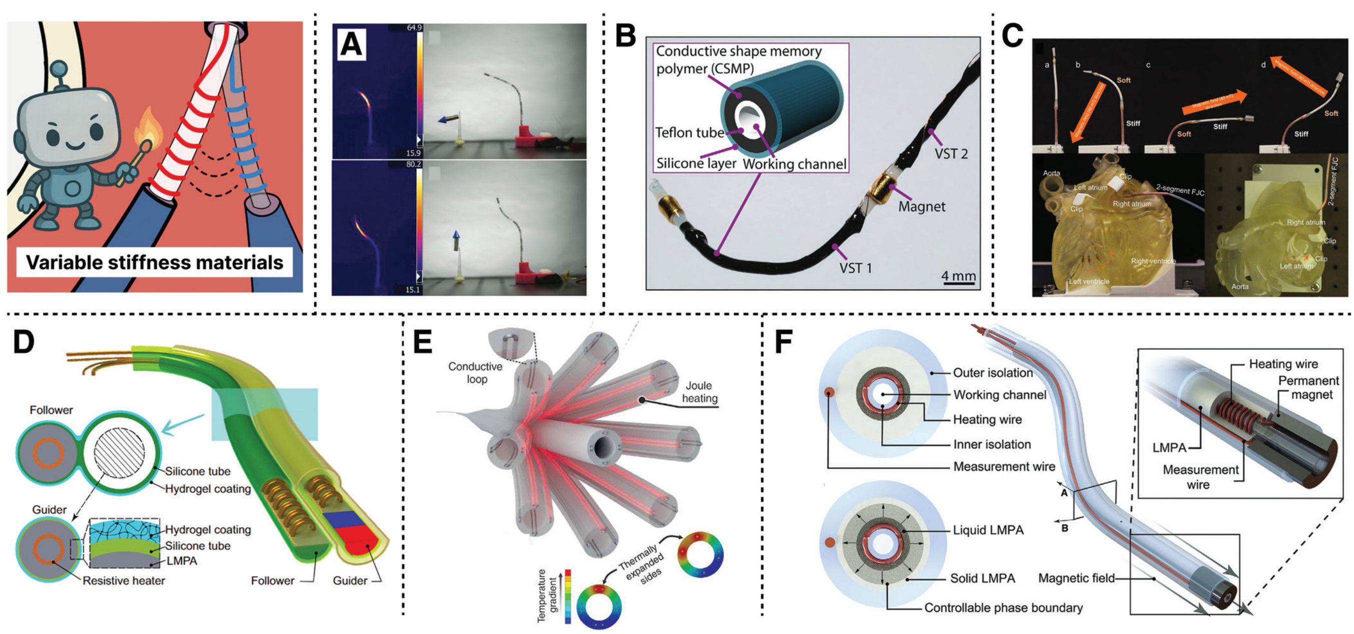

Figure 5. Variable stiffness materials. (A) Thermoset SMP catheter with fast response. Reproduced with permission from Mattmann et al.[44] Copyright 2021, Wiley-VCH GmbH. (B) Conductive SMP thread with magnetic control. Reproduced with permission from Piskarev et al.[45] Copyright 2022, Wiley-VCH GmbH. (C) LMPA catheter enabling FTL actuation. Reproduced with permission from Mao et al.[46] Copyright 2024, Springer Nature. (D) Fiber-jamming catheter for fast stiffening. Reproduced with permission from Sun et al.[47] Copyright 2025, The American Association for the Advancement of Science. (E) Thermally drawn catheter with embedded features. Reproduced with permission from Abdelaziz et al.[48] Copyright 2024, The American Association for the Advancement of Science. (F) Variable stiffness catheter capable of performing ophthalmic surgery. Reproduced with permission from Lussi et al.[15] Copyright 2021, Wiley-VCH GmbH.

Overall, the key challenges in current variable-stiffness catheter technologies include substantial energy requirements for thermal actuation, limited stiffness-tuning ranges in some polymeric materials, difficulty integrating sensing and actuation components, and unresolved concerns about long-term biocompatibility. In particular, the long-term stability of SMPs and LMPAs under repeated actuation in blood remains uncertain, as hydrolytic degradation or particle release may induce inflammation or thrombosis. Further in vitro and in vivo evaluations, including fatigue and hemocompatibility testing, are required to verify their safety for chronic intravascular applications.

4. Catheter sensors

The incorporation of advanced sensing modalities into intravascular catheter systems is critical to enabling precise, safe, and adaptive endoluminal interventions. By providing real-time information on anatomical structures, physiological conditions, and catheter–tissue interactions, sensing technologies lay the foundation for enhanced procedural guidance, autonomous navigation, and closed-loop control in increasingly complex clinical scenarios[19]. This section focuses on the most common intravascular sensing modalities and their latest research applications, including IVUS, OCT, FBG sensors, and MEMS.

4.1 Intravascular ultrasound

IVUS has emerged as 1 of the most mature and effective intraluminal imaging modalities for real-time assessment of vascular structures, particularly in the context of atherosclerosis diagnosis and interventional guidance. At its core, IVUS employs high-frequency ultrasound transducers to generate cross-sectional images of vessel walls, providing detailed visualization with axial resolution[51]. Several commercial IVUS systems exemplify the advancement of this technology. For instance, the Philips Eagle Eye Platinum catheter utilizes a digital transducer with advanced features like ChromaFlo[52] for flow visualization; Boston Scientific's OptiCross[53] series offers high-resolution rotational imaging for coronary assessment; and Insight Lifetech TrueVision[54] system integrates a catheter with a high frame rate console, representing a new generation of high-frequency IVUS platforms.

To overcome the challenges of miniaturization and mechanical complexity in high-frequency ultrasound systems, various research strategies have been proposed. For instance, Xu et al.[55] developed a mechanical scanning IVUS system. Their design included a motion-compensation algorithm that corrected for nonlinear scanning distortion, achieving a spatial resolution of 51 μm and an imaging depth of 8 mm. Hou et al. (Figure 6A)[56] introduced a distal micromotor-driven side-looking IVUS catheter. This eliminated the friction-induced nonuniform rotational distortion (NURD) typically seen in traditional designs, thereby improving maneuverability in curved vessels. Similarly, Peng et al. (Figure 6B)[57] proposed a synchronous electromagnetic micromotor for IVUS applications, achieving high rotational stability with angular errors below 7 ° and a rotation speed of up to 275 revolutions per second.

NURD has also been addressed through sensing and correction. Han et al. (Figure 6C)[58] developed a miniature 50 MHz rotary ultrasonic encoder that directly measures angular position during catheter rotation. Liu et al. (Figure 6D)[59] presented a dual-element IVUS catheter featuring 2 back-to-back transducers operating at 40 MHz. This configuration enabled complementary imaging: when distortion or signal loss occurred on 1 side due to vessel curvature or tissue obstruction, the opposing transducer could provide undistorted data.

More recently, robotic and magnetically actuated IVUS systems have opened new possibilities for imaging in highly tortuous vessels. Yang et al. (Figure 6E)[9] developed a dual-mode magnetic IVUS robot that combines static magnetic steering and dynamic magnetic beam scanning, allowing precise tip navigation and high-speed imaging. Their catheter design integrates a permanent magnet with a single-element transducer, enabling real-time ultrasound acquisition and controllable positioning using external magnetic fields. This innovation eliminates mechanical shafts entirely, significantly reducing the risk of NURD.

Collectively, these approaches improve IVUS resolution, mechanical stability, and imaging flexibility through complementary strategies. Whether through mechanical optimization, dual-transducer redundancy, solid-state transducer integration, or robotic actuation, each study offers a unique solution to the technical challenges that continue to shape the future of IVUS systems.

4.2 Optical coherence tomography

OCT is an intravascular imaging technique that utilizes near-infrared light to provide real-time, high-resolution visualization of vascular structures. OCT catheters consist of a rotating optical fiber within a transparent sheath, delivering wavelength light to achieve penetration depths of 0.1–2 mm[66]. With axial resolutions typically ranging from 1 to 10 μm and lateral resolutions as fine as 5 μm, OCT catheters outperform IVUS catheters in resolving microstructures such as thin fibrous caps, lipid pools, cholesterol crystals, and stent struts, which are critical for identifying vulnerable plaques and evaluating stent deployment outcomes[67]. Commercial OCT catheters include Abbott's Ilumien Optis[68] integrated with Ultreon software for AI-assisted image interpretation, and Conavi Medical's Novasight Hybrid[69], combining OCT and IVUS in a single catheter.

Modern intravascular OCT catheter designs aim for compactness and flexibility. Some OCT catheters[70] have diameters of ≤1 mm, though some novel designs report probes as thin as 0.457 mm using 3D-printed freeform optics or even 0.52 mm using monolithic ball-lens microprobes[69]. These ultrathin designs enable imaging in extremely narrow vessels or lumens (eg, small airways, deep brain)[61] without inducing trauma.

Functional advances are also evident in catheter scanning mechanisms. Probe innovations include meta-lenses that eliminate spherical and astigmatic aberrations, achieving diffraction-limited performance over an extended depth of focus[71]. Traditional torque coil systems suffer from NURD, especially in tortuous vessels. Wang et al. (Figure 6F)[60] developed a miniature piezoelectric-driven fiber optic slip ring (FOSR) probe, achieving 360 ° scanning at 10,000 rpm within a 0.85 mm form factor. Similarly, Zhang et al.[72] presented a pneumatic OCT probe with a turbine scanner reaching 446 revolutions per second, offering distortion-free imaging even in tortuous bronchial lumens. They also developed a Magnetic-OCT system[73] for motor-free telerobotic endomicroscopy, enabling steerable and programmable imaging in complex, curved, and localized areas. Beyond diagnosis, OCT is expanding toward theranostic applications. Yuan et al. (Figure 6G)[61] reported an OCT microneedle integrating 800 nm imaging and 1448 nm laser ablation in a 580 μm probe for real-time deep brain tumor imaging and treatment.

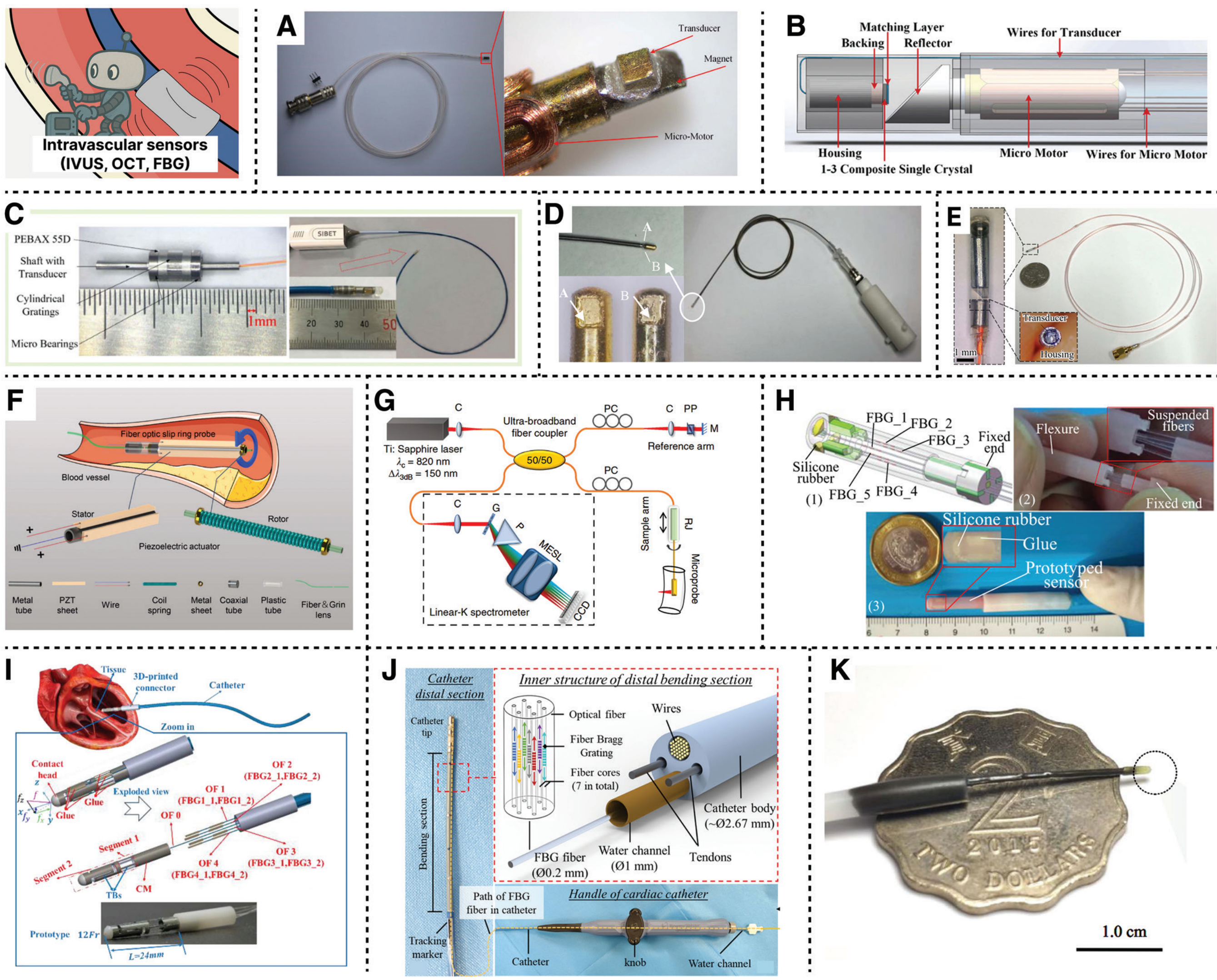

Figure 6. Intravascular sensors. (A) Micromotor-driven side-looking ultrasound catheter. Reproduced with permission from Hou et al.[56] Copyright 2022, IEEE. (B) Electromagnetic micromotor for stable IVUS rotation. Reproduced with permission from Peng et al.[57] Copyright 2019, IEEE. (C) Rotary ultrasonic encoder for NURD correction. Reproduced with permission from Han et al.[58] Copyright 2021, IEEE. (D) A dual-element catheter enabling redundant imaging. Reproduced with permission from Liu et al.[59] Copyright 2023, IEEE. (E) Magnetically steered IVUS robot with scanning. Reproduced with permission from Yang et al.[9] Copyright 2025, IEEE. (F) Piezoelectric OCT scanner with FOSR. Reproduced with permission from Wang et al.[60] Copyright 2023, IEEE. (G) OCT microneedle with laser ablation function. Reproduced with permission from Yuan et al.[61] Copyright 2020, The American Association for the Advancement of Science. (H) Flexure FBG force sensing catheter. Reproduced with permission from Li et al.[62] Copyright 2020, IEEE. (I) Miniature FBG sensor with compliant structure. Reproduced with permission from Wang et al.[63] Copyright 2025, IEEE. (J) MRI-compatible FBG catheter for shape feedback. Reproduced with permission from Dong et al.[64] Copyright 2022, IEEE. (K) Magnetically actuated FBG-enabled continuum robot. Reproduced with permission from Zhang et al.[65] Copyright 2024, Springer Nature.

Challenges persist, particularly in improving blood tolerance and imaging depth. Efforts include polarization-sensitive and adaptive-optics OCT, as well as improved swept-source systems for enhanced signal robustness. Integration with AI and robotic platforms is actively pursued to enable intelligent, image-guided navigation and intervention.

4.3 Fiber Bragg grating

FBG sensors have emerged as a promising technology for enabling high-resolution within minimally invasive intravascular catheters[74]. By reflecting a specific Bragg wavelength in response to strain and temperature changes, FBGs provide real-time feedback on mechanical interactions without relying on electronic components, making them inherently compatible with magnetic resonance imaging (MRI) and other electromagnetically noisy environments[75].

Li et al.[76] demonstrated a triaxial force sensor utilizing an FBG triaxial force sensor with integrated flexure structure, achieving force resolutions of 2.13–2.52 mN for transverse and 23.12 mN for axial directions. Simulation and in vitro vessel phantom tests confirmed the effective decoupling of force and temperature effects. Subsequently, Li et al. (Figure 6H)[62] also developed a 3D-printed FBG sensor optimized for robustness and high resolution (0.52–0.64 mN), achieving <3% RMS error in dynamic force measurements and improved temperature compensation across 25–50 °C. More recently, Wang et al. (Figure 6I)[63] introduced a miniaturized FBG sensor with a compliant mechanism and an integrated laser-ablation channel, reporting force resolutions of 4.7–11.6 mN across 3 axes. Their use of a reduced-order global transfer matrix method enabled rapid modeling and optimization. The sensor supported ex vivo cardiac ablation, confirming its applicability in functional surgical tasks.

In robotic settings, FBGs have been employed for shape sensing and closed-loop feedback. Dong et al. (Figure 6J)[64] integrated a multicore FBG array into a steerable MRI catheter, achieving real-time shape reconstruction with 1.53 mm tip accuracy and enabling autonomous navigation in simulated ablation procedures. Similarly, Zhou et al.[13] reported a fiber robot that combines macro-scale tendon-driven motion and microscale precision via integrated optical fiber waveguides, enabling decoupled multiscale manipulation in endoluminal contexts. Abdelaziz et al.[48] developed a thermal actuated fiberbot with <50 μm positioning accuracy for laparoscopic navigation and molecular tissue ablation, showcasing scalable fabrication via fiber drawing. Zhang et al. (Figure 6K)[65] further demonstrated a 0.95 mm continuum robot with magnetic steering and embedded optical fiber array for imaging, ablation, and drug delivery, offering <30 μm motion precision in constrained anatomical pathways.

Despite these advances, integrating FBGs into submillimeter or highly flexible catheter systems poses challenges, such as maintaining stable fiber alignment under deformation and preserving signal fidelity during physiological motion.

4.4 MEMS

MEMS (Figure 7) have emerged as a transformative approach to functionalize intravascular catheters by integrating microscale sensors and actuators onto compact, low-power platforms[20]. Their capacity for high-resolution, real-time monitoring makes them ideal for applications requiring precise measurement of pressure, flow, temperature, and mechanical interaction forces[80].

Recent developments illustrate the breadth of MEMS integration into catheter systems. For instance, Kwon et al. (Figure 7A)[77] reported a battery-less wireless implant incorporating silicon nanomembrane sensors for continuous trimodal monitoring of vascular pressure, flow, and temperature, achieving high sensitivity under in vivo conditions. Han et al. (Figure 7B)[14] demonstrated soft multilayer catheter integrated arrays capable of simultaneous electrical mapping, pressure sensing, and electroporation, offering conformal tissue contact and dynamic adaptability. The mechanical interface between MEMS sensors and soft tissue remains critical. Shen et al. (Figure 7C)[78] introduced a flounder-shaped stretchable electrode system for pulsed-field ablation, achieving uniform electric fields and mechanical stability under 87% compression. This configuration enhanced ablation depth and reduced electrode failure rates to below 0.1%. Meanwhile, Xue et al. (Figure 7D)[79] adapted balloon-assisted 3D MEMS electrode arrays for colon electrophysiology, capturing pacemaker-like signals with signal-to-noise ratios exceeding 25 dB in vivo.

In addition to sensing, MEMS systems are increasingly used for actuation and localized therapy. Singh et al.[81] developed an electroceutical catheter using retractable nitinol electrodes to deploy a voltage-activated adhesive patch, sealing 2 mm vascular defects under 350 mm Hg burst pressure and tolerating over 20,000 deformation cycles. The patch demonstrated minimal electrical leakage and stable adhesion under blood flow. Huang et al. (Figure 7E)[20] emphasized modular integration of sensing, imaging, and therapy through catheter platforms embedded with MEMS arrays, suggesting synergistic designs for neural, vascular, and gastrointestinal applications.

The development of fully integrated smart catheters depends not only on advanced materials and sensing modules but also on reliable power transmission and data telemetry within the confined intravascular environment. Inductive coupling remains the leading approach for wireless power transfer, enabling safe milliwatt-level delivery through tissue, although alignment and depth constraints persist. Optical energy transmission and

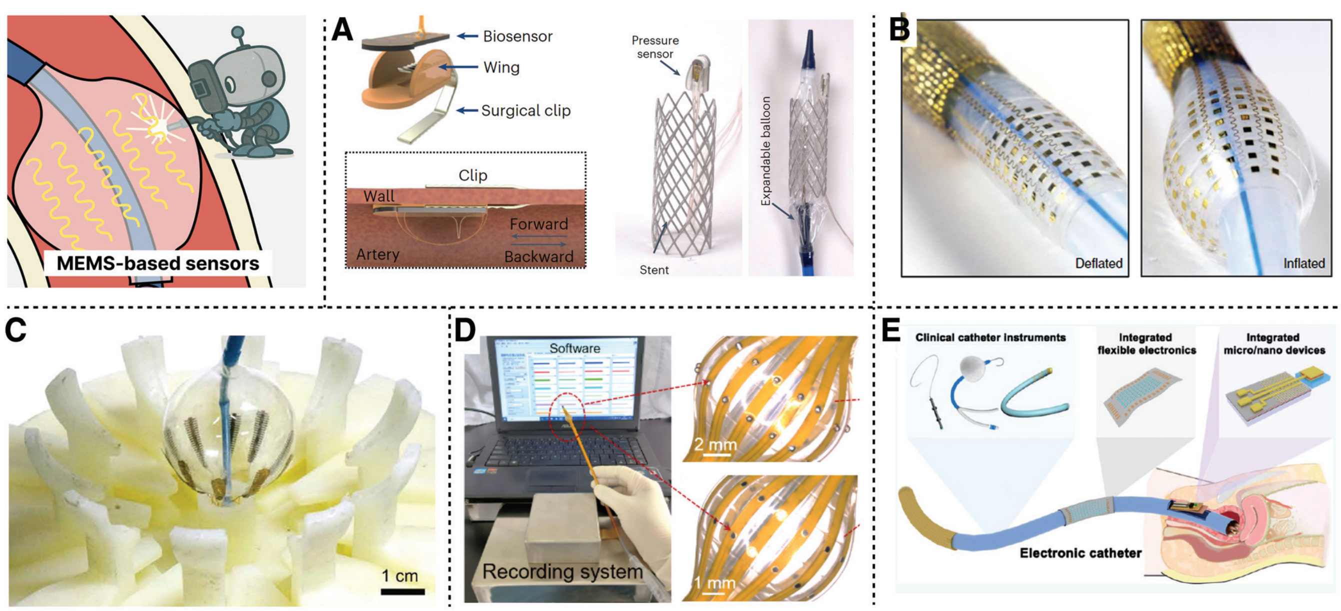

Figure 7. MEMS sensors. (A) Wireless nanomembrane sensors for vascular monitoring. Reproduced with permission from Kwon et al.[77] Copyright 2023, Springer Nature. (B) Multilayer catheter with mapping and electroporation. Reproduced with permission from Han et al.[14] Copyright 2020, Springer Nature. (C) Stretchable electrodes for pulsed field ablation. Reproduced with permission from Shen et al.[78] Copyright 2024, The American Association for the Advancement of Science. (D) Balloon-assisted MEMS for colon electrophysiology. Reproduced with permission from Xue et al.[79] Copyright 2024, Elsevier. (E) Modular catheter integrating sensing and therapy. Reproduced with permission from Huang et al.[20] Copyright 2024, American Chemical Society.

communication via fiber optics provide simultaneous power and high-speed data transfer but require careful management of bending losses. Battery-free energy harvesting from intravascular flow, vibration, or ambient radio frequencies, such as triboelectric nanogenerators[82], offers a promising route to eliminate bulky batteries. Integrating these technologies may enable multifunctional, miniaturized, and biocompatible catheters for next-generation clinical applications.

5. Actuated catheters

Actuated catheters (Figure 8) represent a transformative advancement in intravascular and minimally invasive medical procedures, enabling precise therapy and diagnosis within the human body[18]. These catheters transcend traditional passive conduits by integrating active functionalities such as ablation, thrombectomy, and steering.

5.1 Ablation catheter

Ablation catheters are designed to deliver energy precisely to targeted tissues, allowing clinicians to eliminate abnormal or diseased structures with minimal invasiveness[88]. In cardiology, they are central to treating arrhythmias by selectively destroying ectopic foci or reentrant pathways, enabling high-precision intervention inside the heart. Representative systems include the Farapulse pulsed field ablation system by Boston Scientific[89], offering nonthermal lesion formation with high tissue selectivity; Medtronic's Arctic Front Advance cryoballoon[90], which enables circumferential pulmonary vein isolation with a single application; and the Thermocool Smart Touch SF catheter from Biosense Webster[91], integrating contact force sensing with open irrigation for precise thermal ablation.

Radiofrequency (RF) ablation remains the most widely used modality. Nguyen et al. (Figure 8A)[83] integrated transparent silicon carbide electrodes into an endoscopic platform, combining excellent optical visibility with stable electrical performance. At 450 kHz, their system raised tissue temperature to 80 °C while supporting real-time feedback and multimodal sensing. Pulsed field ablation, which relies on nonthermal irreversible electroporation, is emerging as a promising alternative. Xu et al. (Figure 8B)[84] developed a catheter with microelectrodes that produced precise lesions in large-animal hearts using 300 V pulses and achieved lesion widths as narrow as 3.8 mm, thereby improving safety in complex anatomies. Accurate energy delivery depends on robust intraoperational sensing. Koh et al.[92] introduced ultrathin injectable sensors that measure temperature, thermal conductivity, and heat capacity in situ during RF and cryoablation. Their multilayer polymer needle provided depth-resolved thermal maps, showing a strong correlation between thermal profiles and lesion transmurality.

Progress in materials, sensing, and lesion assessment is steadily moving ablation technology toward multifunctional, intelligent catheters that offer real-time feedback, tighter energy control, and greater procedural safety—key steps toward more effective and tailored intravascular therapies.

5.2 Thrombectomy catheter

Thrombectomy mechanisms in intravascular catheters aim to mechanically remove resistant obstructions, such as calcified plaques or organized thrombi, especially when standard

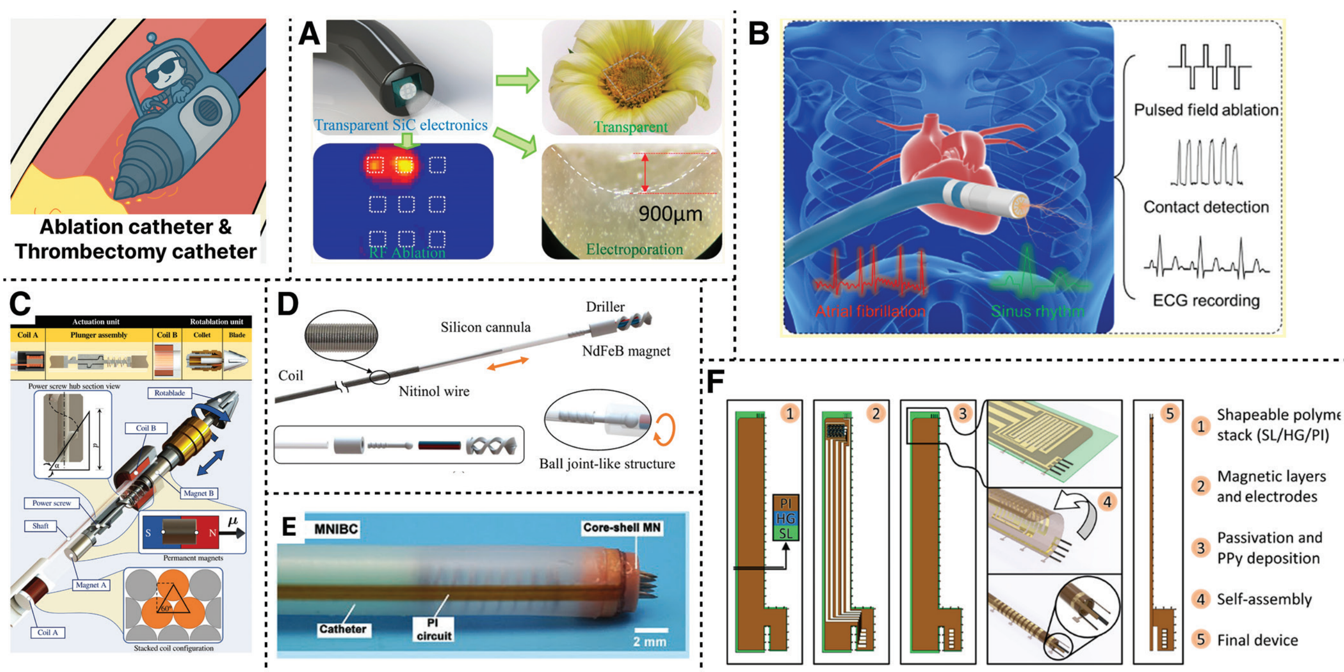

Figure 8. Ablation catheter and thrombectomy catheter. (A) Transparent SiC electrode for RF ablation. Reproduced with permission from Nguyen et al.[83] Copyright 2022, American Chemical Society. (B) Low-voltage microelectrode for pulsed ablation. Reproduced with permission from Xu et al.[84] Copyright 2023, Wiley-VCH GmbH. (C) Magnetically actuated rotablation catheter system. Reproduced with permission from Heunis et al.[85] Copyright 2022, IEEE. (D) Driller tipped the guidewire with magnetic steering. Reproduced with permission from Yang et al.[86] Copyright 2022, IEEE. (E) Microneedle catheter for sensing and therapy. Reproduced with permission from Huang et al.[87] Copyright 2023, Wiley-VCH GmbH. (F) Microcatheter with actuated digits and tracking. Reproduced with permission from Rivkin et al.[12] Copyright 2021, The American Association for the Advancement of Science.

angioplasty is ineffective. Common applications include atherectomy procedures for restoring vessel patency in chronic total occlusions or severely calcified lesions. Commercialization technologies include rotational (eg, Rotablator[93]), orbital (eg, Diamondback 360[94]), and directional atherectomy, each using different high-speed or orbiting cutters.

Heunis et al. (Figure 8C)[85] developed a magnetically actuated rotablation catheter featuring a spring-loaded mechanism that achieves a maximum axial force of 2.63 N and torque of 5.69 mN·m. Their device demonstrated effective plaque removal, reducing the stenosis cross-sectional area by up to 35%, using interchangeable drill bits activated by internal electromagnetic coils (EMNS). Yang et al. (Figure 8D)[86] proposed a driller-tipped guidewire integrated with magnetic navigation and ultrasound imaging, enabling real-time control for penetrating chronic total occlusions. Their system combined directional and rotational magnetic fields to switch between steering and drilling modes, achieving successful unclogging within tissue-mimicking vascular phantoms. Huang et al. (Figure 8E)[87] developed a Petromyzontidae-inspired microneedle-integrated bioelectronic catheter featuring multifunctional microneedle tips capable of biochemical sensing, electroporation, and drug delivery. Khalil et al.[95] introduced a helical microrobot for mechanical clot removal via magnetic rubbing. The in vitro experiments quantified a clot-removal rate of −0.885 mm³/min at 35 Hz, approximately 5 times more effective than conventional streptokinase thrombolysis (−0.17 mm³/min).

On the other hand, Mao et al.[46] presented a millimeter-scale magnetic continuum robot capable of “follow-the-leader” deployment via tip-steered elongation. Their design enabled safe navigation through tortuous lumina and morphing into functional configurations at the target site. The robot employed dual-phase transition materials for stability and mobility and demonstrated in vivo capabilities such as knotting, pressure sensing, and instrument delivery. Rivkin et al. (Figure 8F)[12] reported a self-assembled microcatheter with integrated actuated digits and a magnetic sensor. The device, with a diameter of only 120 µm, supports fluid delivery, micromanipulation, and real-time magnetic tracking. It demonstrated clot manipulation and precise liquid administration within ex vivo and artificial vascular models.

The thrombectomy catheter systems require atraumatic, precise control in complex vascular anatomy. While imaging guidance and robotic assistance improve surgical safety, limitations remain, including incomplete capture, vessel trauma, and poor visibility. Future designs are expected to emphasize miniaturization, force feedback, and multifunctionality to enable intelligent and adaptive intervention in complex vascular environments.

5.3 Steerable catheter

Steerable catheters (Figure 9) are intravascular tools equipped with tip actuation mechanisms that provide enhanced directional control, enabling precise navigation in tortuous vascular anatomies[99]. Unlike conventional passive systems that rely on guidewires and torque transfer, steerable platforms improve access to challenging targets, such as the cerebral vasculature and coronary bifurcations[100]. Commercially, systems such as the SwiftNINJA[101] microcatheter offer dual-directional 180 ° tip deflection for rapid vessel selection, while NAVISTAR[97] catheters integrate electroanatomical mapping with steerable control for precise ablation during electrophysiological procedures.

Pull wire systems remain a foundational design approach, but achieving high control accuracy and reliability is critical for their clinical effectiveness. Zhou et al. (Figure 9A)[13] developed a macro-micro decoupled continuum robot with a 1 mm outer diameter, integrating tendon-driven macro steering with light-driven micro actuation via liquid crystal elastomer fibers. Their system demonstrated sub-300 µm resolution and a mean trajectory error of just 4.8% in in vivo tympanic membrane procedures, highlighting its potential for precise endoluminal manipulation. Abdelaziz et al.[48] reported a fiber-drawn electrothermal actuator with sub-50 µm positioning accuracy and up to 10 mm/s tip speed. By embedding resistive wires within polymer fibers, this platform achieved planar tip steering suitable for precision surgical navigation. Compared to pull wire systems, concentric tube robots offer superior controllability. Girerd et al. (Figure 9B)[96] proposed a hand-held concentric tube robot capable of 6 degrees of freedom (DOF) tip manipulation with submillimeter accuracy, and demonstrated its effectiveness in simulated percutaneous abscess drainage procedures.

Hydraulically actuated steerable tips offer smooth, continuous motion with high flexibility. Gopesh et al.[101] designed a soft robotic microcatheter with 4 saline-filled microchannels (50 µm) to achieve 3D tip steering without a guidewire, enabling successful embolization in vivo in a porcine model. Rogatinsky et al. (Figure 9C)[97] further expanded this concept by integrating a soft manipulator and deployable stabilization mechanism for intracardiac navigation. Their robotic system could apply up to 1.2 N of radial force and maintain stable contact with dynamic cardiac tissue. Nguyen et al. (Figure 9D)[98] introduced an electricity-free, hydraulically coupled actuator system termed the soft fibrous syringe architecture, capable of tip steering and built-in sensing. Their flexible catheter achieved 4 cm of displacement via fiber-reinforced muscle actuation and demonstrated self-sensing control in a fully soft design. Alternative actuation schemes have advanced the miniaturization and precision control of steerable catheters. Kim et al.[102] Fabricated a magnetorheological elastomer microactuator (0.7 mm diameter) capable of 124 ° bending with only 12 µm positional error, leveraging a novel dip coating process that achieves tunable eccentricity and high repeatability.

The performance of steerable systems hinges on DOF and control strategies[103]. Despite advances, challenges persist in miniaturizing actuation mechanisms without compromising output force, ensuring mechanical durability under cyclic loading, and maintaining biocompatibility[104].

6. Robotic integration

The integration of robotics into functionalized catheter systems marks a critical evolution in endovascular intervention, enabling precise control, real-time navigation, and intelligent feedback in complex vascular environments[105,106]. This section explores key components of robotic integration—including magnetically actuated robots, teleoperation systems, and intravascular robotic navigation—that collectively enhance the performance, autonomy, and clinical applicability of catheter systems.

6.1 Magnetically actuated robot

Magnetically actuated robots (Figure 10) represent a transformative approach for achieving precise, remote, and minimally invasive control of catheters within complex vascular environments. Magnetically steerable robotic systems generally

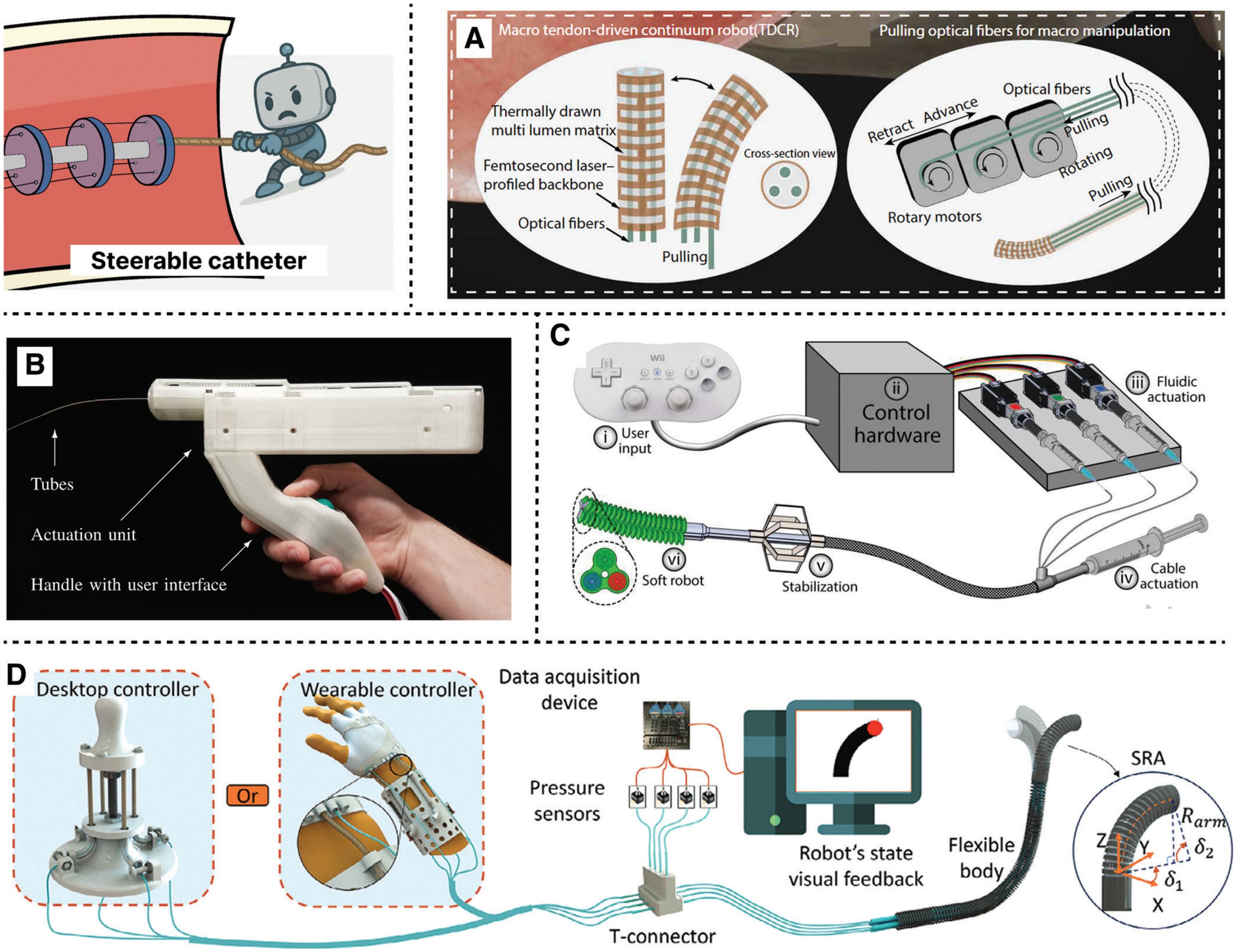

Figure 9. Steerable catheter. (A) Macro-micro continuum robot for precise steering. Reproduced with permission from Zhou et al.[13] Copyright 2024, The American Association for the Advancement of Science. (B) Concentric tube robot with 6 DOF tip. Reproduced with permission from Girerd et al.[96] Copyright 2021, IEEE. (C) Soft intracardiac catheter with deployable stabilizer. Reproduced with permission from Rogatinsky et al.[97] Copyright 2023, The American Association for the Advancement of Science. (D) Hydraulic fiber syringe catheter with self-sensing. Reproduced with permission from Nguyen et al.[98] Copyright 2024, Wiley-VCH GmbH.

comprise a catheter integrated with permanent magnets, soft magnetic materials, or magnetized composites[112]. These devices are actuated through external magnetic fields generated by permanent magnets, EMNS, or MRI scanners. The applied torque and force induce tip deflection or whole-body bending, depending on the device's stiffness and magnetic profile[113]. One notable clinical implementation is the Niobe system by Stereotaxis[114], which utilizes a pair of computer-controlled permanent magnets to generate a dynamic magnetic field around the patient, enabling precise navigation of magnetically tipped catheters with submillimeter accuracy. This technique is particularly promising for intracranial and cardiovascular interventions, where traditional mechanical actuation methods often face limitations due to friction, buckling, or poor steerability.

Kim et al. (Figure 10A)[16] developed ferromagnetic soft continuum robots that achieve omnidirectional bending via programmed magnetic domains, successfully navigating through tortuous cerebrovascular phantoms with diameters below 1 mm. Dreyfus et al. (Figure 10B)[107] introduced a helical magnetic robot with a screw like outer geometry, where tip rotation generated forward propulsion along the vessel wall; the device achieved stable navigation in millimeter-scale cerebral arteries and successfully operated in a live porcine model. Phelan et al. (Figure 10C)[108] demonstrated Lorentz force steering using a quad configuration micro coil catheter compatible with MRI fields up to 7 T, achieving a tip deflection of 110 ° with only 0.44 W of power and without the need for active cooling. Tiryaki et al. (Figure 10D)[109] further investigated magnetic actuation under ultrahigh magnetic fields, showing that guidewires embedded with permanent magnets could achieve torque steering even inside 7T MRI environments via in situ magnetization switching, thus enabling dynamic reconfiguration during navigation. Magnetic navigation systems provide actuation infrastructure for such devices. Hwang et al. (Figure 10E)[110] developed a clinically translatable electromagnetic actuation system combined with a micro robotic guidewire for real-time cardiovascular intervention, demonstrating teleoperated navigation in vivo in swine coronary and renal arteries. Pittiglio et al. (Figure 10F)[111] proposed a cart-mounted permanent magnet system that actuates a ball-chain magnetic catheter, demonstrating a comparable treatment effect to clinical ablation catheters while significantly reducing size.

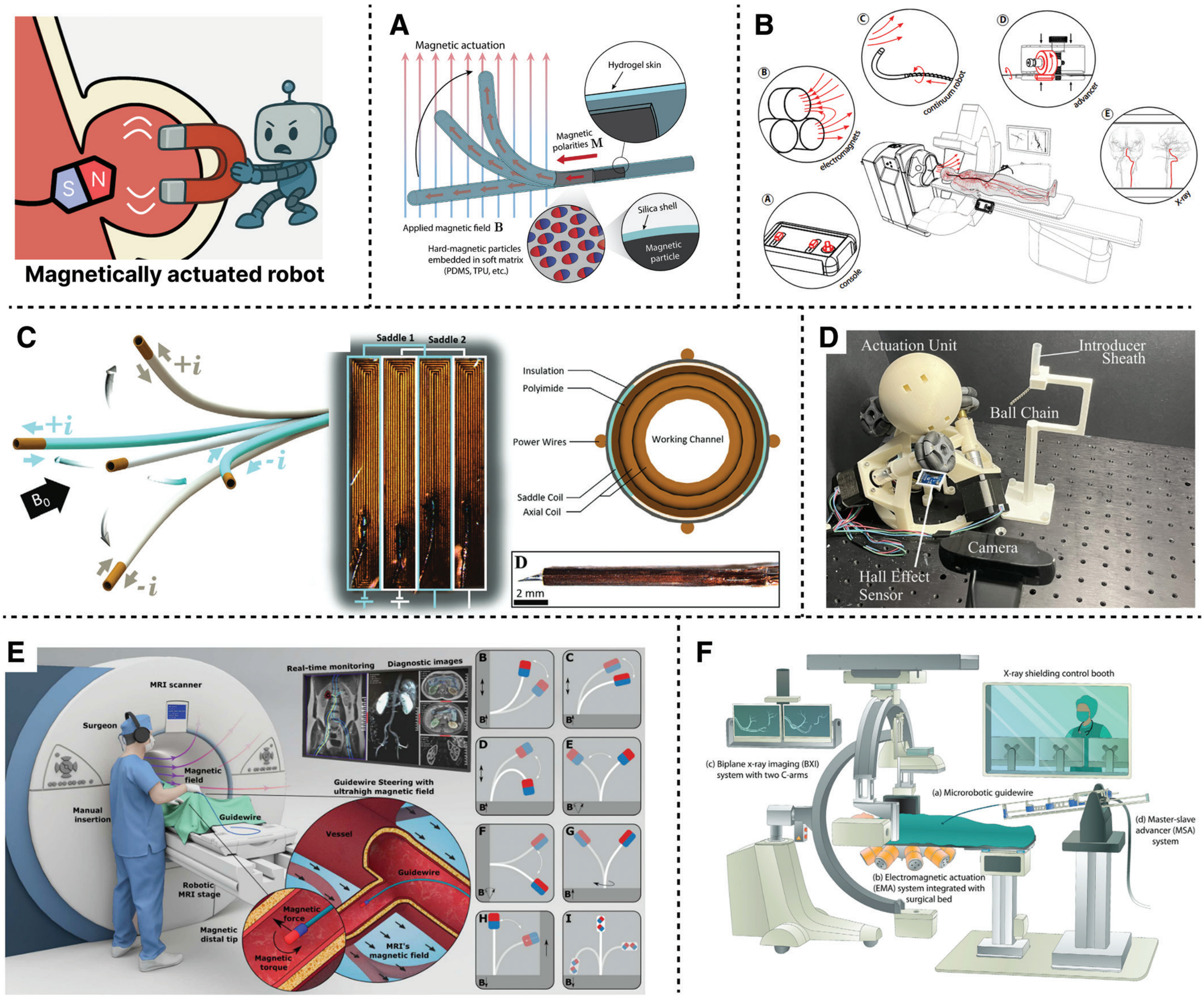

Figure 10. Magnetically actuated robot. (A) Ferromagnetic robot. Reproduced with permission from Kim et al.[16] Copyright 2019, The American Association for the Advancement of Science. (B) Helical robot with screw like propulsion. Reproduced with permission from Dreyfus et al.[107] Copyright 2024, The American Association for the Advancement of Science. (C) Lorentz steered the microcoil catheter for MRI guidance. Reproduced with permission from Phelan et al.[108] Copyright 2022, Wiley-VCH GmbH. (D) Magnetized guidewire enabling in situ steering. Reproduced with permission from Tiryaki et al.[109] Copyright 2023, The American Association for the Advancement of Science. (E) Electromagnetic system with micro robotic guidewire. Reproduced with permission from Hwang et al.[110] Copyright 2022, Wiley-VCH GmbH. (F) Permanent magnet system actuating ball chain catheter. Reproduced with permission from Pittiglio et al.[111] Copyright 2024, IEEE.

Some groups have integrated magnetic steering with therapeutic delivery[115]. Torlakcik et al.[116] engineered a magnetically guided microcatheter with a 15 mm reservoir for iron oxide nanoparticles, demonstrating targeted release within a spinal cord phantom under pulsatile cerebrospinal flow. 86.5% of particle aggregates were successfully delivered at an ejection rate of 200 µL/s. Yan et al.[117] developed a soft tool incorporating a magnetized deformation segment, which achieved 0.06 mm average error in occlusion morphology mapping and selectively crossed microchannels down to 0.2 mm via magneto fluidic interaction in pulsatile flow. Wang et al.[118] expanded this concept to multirobot systems, enabling independent control of over 5 soft magnetic robots in a 3D lumen network by exploiting resistance decoupling between robots.

The main advantage of magnetic steering catheters lies in their use of miniaturized magnetic materials. However, MRI-compatible designs must avoid image artifacts and heating, while permanent magnet systems face spatial constraints and safety concerns. Moreover, achieving precise control in real-time, patient-specific anatomy requires continued advancement in actuation modeling, sensing, and robotic integration.

6.2 Teleoperation robot

Teleoperated control architectures (Figure 11) are central to modern endovascular robotic systems, enabling physicians to perform delicate catheter and guidewire manipulations from remote, radiation shielded consoles. By decoupling the operator from the procedural field, these systems not only mitigate radiation exposure and physical strain but also lay the foundation for long-distance robotic interventions and crossinstitutional telemedicine. Notable commercial platforms include the

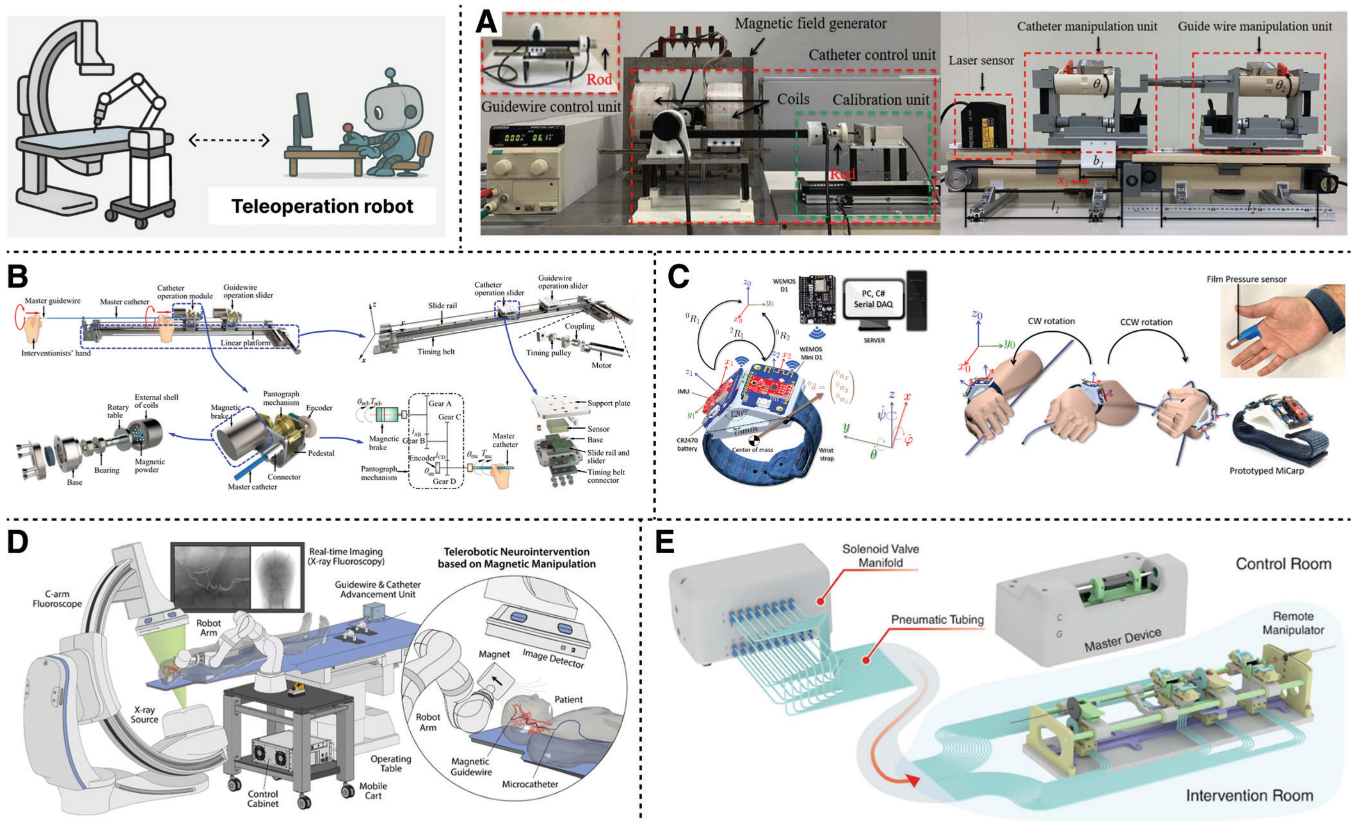

Figure 11. Teleoperation robot system. (A) Robotic catheter with real-time force feedback. Reproduced with permission from Jin et al.[119–121] Copyright 2021, IEEE. (B) Dual hand haptic interface with MR actuators. Reproduced with permission from Bao et al.[122,123] Copyright 2024, IEEE. (C) Sensor-fused system for rotational tracking. Reproduced with permission from Hooshiar et al.[124,125] Copyright 2022, IEEE. (D) Telerobotic system for neurovascular interventions using magnetic navigation. Reproduced with permission from Kim et al.[126] Copyright 2022, The American Association for the Advancement of Science. (E) Pneumatic teleoperation platform for robotic angioplasty. Reproduced with permission from Dagnino et al.[127] Copyright 2023, IEEE.

CorPath GRX[128,129] by Siemens, which is widely used in coronary and peripheral vascular procedures. The R-One[130] system from Robocath delivers CE-certified precision and offers intuitive control for PCI. In addition, the RoboAngio[131] system developed by Abrobo has supported numerous remote vascular interventions and incorporates force feedback to enhance surgical dexterity and tactile awareness.

Conventional teleoperation systems rely on user inputs to drive linear and rotational motions at the catheter tip, often through mechanical or electromagnetic transmission. Jin et al. (Figure 11A)[119–121] developed a robotic catheter system with integrated force sensing and tactile feedback, allowing the operator to detect vessel collision forces in real-time. Their design distinguished between contact and inertial forces using a custom sensor array, improving procedural safety. Addressing the limitations of standard joystick interfaces, Bao et al. (Figure 11B)[122,123] introduced a dual-hand haptic system that preserves the surgeon's habitual handling of catheters and guidewires. Their interface achieved closed-loop force and torque feedback via MR fluid actuators and pantograph transmission, delivering resolution of 0.06 N and 0.07 mN·m, respectively, with 5 Hz control bandwidth during animal studies.

Hooshiar et al. (Figure 11C)[124,125] proposed an inertial free orientation measurement framework for teleoperated catheterization. By integrating stereo accelerometry and neural network fusion, their system captured rotational motion with a mean absolute error of 1.7 ° and enabled high-frequency sampling at 117 Hz. Kim et al. (Figure 11D)[126] demonstrated a magnetically guided robotic platform for neurovascular interventions, combining a 7 DOF robotic arm with steerable magnetic guidewires and motorized catheter advancement. Their system enabled real-time manipulation under fluoroscopy and achieved successful embolization and thrombectomy in porcine models, navigating tortuous vasculature otherwise inaccessible to manual methods. Dagnino et al. (Figure 11E)[127] reported an in vivo evaluation of a pneumatic robotic platform that performed robotic angioplasty in porcine arteries. The system combined ergonomic teleoperation with dynamic haptic feedback and virtual fixtures, achieving a 100% procedural success rate and reducing vessel trauma compared with manual navigation.

As robotic teleoperation converges with intelligent assistance, multimodal sensing, and networked connectivity, it is poised to transform interventions into standardized, remotely operable procedures, thereby broadening access to specialized care across geographic and institutional settings.

6.3 Robotic navigation

Accurate and responsive navigation (Figure 12) is fundamental to the safe and effective deployment of intravascular robotic systems. As catheter interventions increasingly target deep and tortuous anatomical regions such as cerebral arteries or the aortic arch, robust navigation technologies have become indispensable[137]. These systems provide real-time localization and trajectory control, minimizing procedural risks while supporting autonomous or semiautonomous operation. Representative

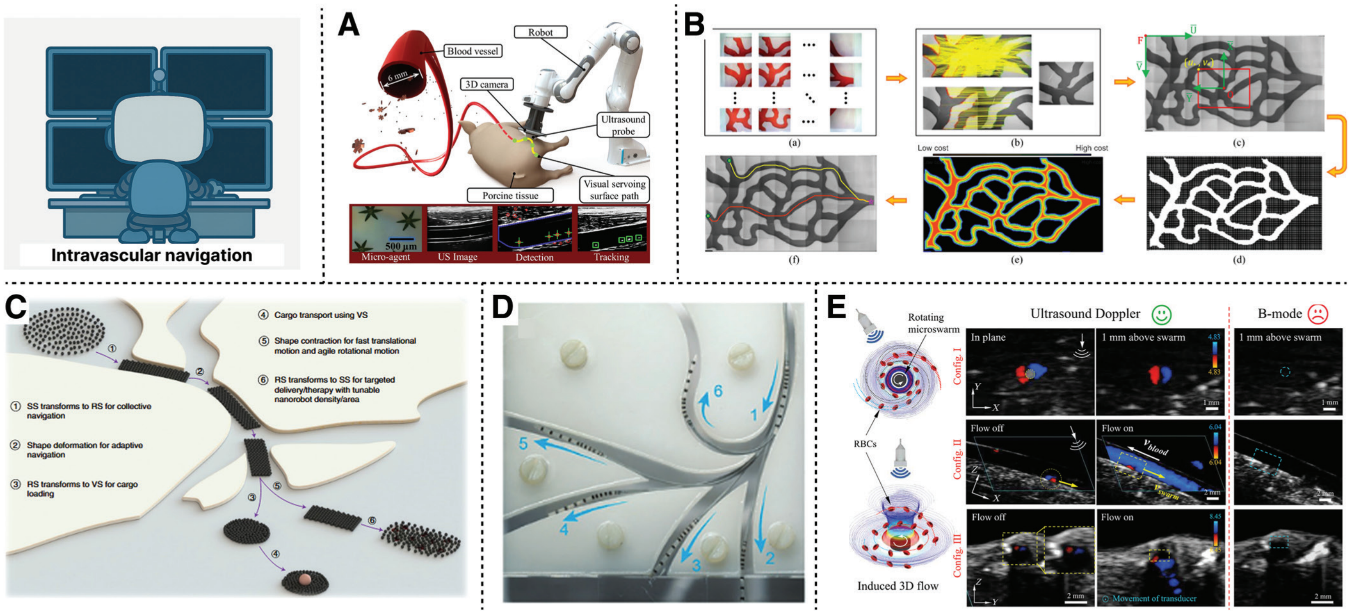

Figure 12. Intravascular navigation. (A) Ultrasound integrated electromagnetic tracking with servo control. Reproduced with permission from Šuligoj et al.[132] Copyright 2022, IEEE. (B) Mobile coil microrobot navigation with visual feedback. Reproduced with permission from Yang et al.[133] Copyright 2021, IEEE. (C) Adaptive swarm navigation via deep learning. Reproduced with permission from Yang et al.[134,135] Copyright 2022, Springer Nature. (D) Magnetically guided microcatheter for nanoparticle delivery. Reproduced with permission from Torlakcik et al.[116] Copyright 2024, Wiley-VCH GmbH. (E) Doppler localized microrobots navigating against flow. Reproduced with permission from Wang et al.[136] Copyright 2021, The American Association for the Advancement of Science.

commercial solutions include Philips' VesselNavigator[138], which overlays preoperative computed tomography angiography/magnetic resonance angiography data onto live fluoroscopy to guide complex vascular access. Therenva's EndoNaut system[139] enables 3D fusion of intraoperative images, allowing for precise catheter tracking. Additionally, Centerline Biomedical's IOPS platform[140] offers radiation-free 3D navigation using electromagnetic localization.

Fluoroscopic imaging remains the clinical gold standard, offering widespread accessibility and continuous visualization. However, Vandini et al.[141] point out that the inherent 2D projection and poor soft-tissue contrast limit fluoroscopy's utility, especially during dynamic or complex interventions. To address these challenges, they developed a guidewire-tracking algorithm using segment-like features that achieved an F1 score of 92% under large deformation conditions, outperforming prior methods. Electromagnetic tracking offers an alternative, enabling real-time 3D localization of embedded sensors without requiring a direct line of sight. Suligoj et al. (Figure 12A)[132] demonstrated ultrasound-integrated robotic EM tracking of microagents with 99.8% tracking accuracy, leveraging visual servoing for catheter navigation under breathing motion and flow simulations. MRI navigation presents another promising modality[142,143]. Azizi et al.[144] utilized the fringe field of a clinical MRI scanner to generate directional magnetic gradients of up to 2 T/m for robotic guidewire navigation. This approach enabled selective pulling of microguidewires through multibifurcated and tortuous vessels that were otherwise inaccessible by manual pushing, demonstrating in vivo feasibility in swine models. Felfoul et al.[145] achieved closed-loop commutation control of an MRI-powered rotor actuator using interleaved imaging and propulsion sequences. Their system delivered a peak force of 9.4 N, representing a key step toward MRI-driven robotic actuation within clinical environments.

At the microscale, Yang et al. (Figure 12B)[133] implemented autonomous navigation of magnetic microrobots in large workspaces using a mobile coil system. Their approach combined real-time visual feedback with modified A* planning and model predictive control, enabling microrobots to traverse maze-like environments of up to 230 mm in diameter. Expanding upon this, Yang et al. (Figure 12C)[134,135] leveraged deep learning to endow microrobot swarms with environment-adaptive distribution planning. Their framework enabled microrobots to autonomously reconfigure in response to obstacles, enabling fully autonomous navigation to dynamically assigned targets. Magnetically guided microcatheters have also shown potential for targeted delivery. Torlakcik et al. (Figure 12D)[116] developed a 1-mm-diameter microcatheter capable of magnetically steered intrathecal delivery of nanoparticle swarms. Numerical simulations and in vitro spinal cord phantom experiments confirmed controlled deployment against physiological counterflows. Complementary to this, Wang et al. (Figure 12E)[136] demonstrated that rotating magnetic microrobot swarms in blood can be localized using ultrasound Doppler imaging. The Doppler signals induced by collective microrobot motion enabled indirect localization even when imaging planes were misaligned, facilitating upstream navigation against blood flow at velocities up to 5.97 mm/s. Autonomous control strategies are also emerging. Fagogenis et al.[146] introduced a robotic catheter using haptic vision for autonomous wall following navigation within a beating heart. Their system achieved 99% success rate in navigating from the apex to the aortic valve, performing comparably to expert clinicians while reducing reliance on fluoroscopy.

In summary, advances in fluoroscopy enhanced feature tracking, EM and MRI localization, ultrasound guided microscale tracking, and learning-based swarm control are collectively transforming intravascular navigation from passive guidance to intelligent, autonomous execution. Each modality offers distinct advantages, and their fusion facilitates the development of robust, adaptive navigation systems in future endovascular robotics.

7. Discussion

Over the past decade, endovascular technology has advanced from single-function catheters to robot-assisted systems capable of sensing, actuation, and intelligent control. Figure 13 presents a concise future roadmap, outlining the progressive evolution from conventional catheters toward fully functionalized systems that integrate materials, sensors, actuators, and robotics. The roadmap highlights key performance improvements, such as higher biocompatibility, multimodal sensing, soft and energy-efficient actuation, and semiautonomous operation, that together define the next generation of intelligent endovascular platforms.

In addition, a new quantitative comparison table (Table 1) provides a clear performance benchmark between representative commercial and emerging endovascular systems. The table compares material stiffness, sensor resolution, actuation speed, and size/compatibility across the major categories of materials, sensors, actuation mechanisms, and robotic integration. The final column, Comparative Advantages of Emerging Systems, highlights the primary improvements of research prototypes over clinical-grade devices, outlining the technological trajectory toward adaptive, intelligent, and multifunctional catheter platforms.

Proof-of-concept solutions now exist for nearly every subsystem: biocompatible coatings, variable-stiffness backbones, high-density FBG shape sensors, MEMS-based force arrays, and both teleoperated and magnetically actuated mechanisms[20,80,147,148]. Yet these components are often demonstrated in isolation. Future catheter platforms will require a unified architectural framework that codesigns materials, electronics, and control algorithms within the constraints of a catheter lumen. Key challenges include achieving high-density wiring or optical routing without compromising flexibility, ensuring electromagnetic compatibility among mixed-signal modules, and managing heat dissipation to maintain endothelial safety.

Variable stiffness designs have already demonstrated stiffness changes spanning more than 2 orders of magnitude with sub-10-second response times[74,149]. Embedding such mechanisms into closed-loop systems that sense wall stress and dynamically adjust compliance could reduce the risk of vessel perforation and improve distal navigation. However, this vision demands high-bandwidth, biocompatible actuation and power delivery systems.

Current navigation systems can stream data from fluoroscopy, IVUS/OCT, and electromagnetic tracking[66,75,150]. However, fusing these heterogeneous data sources into a coherent, latency-free digital representation of catheter–vessel interaction remains an open problem. Real-time autonomy will depend not only on solving this fusion challenge but also on developing large, annotated, procedure-specific datasets and robust validation pipelines that meet regulatory standards for safety-critical AI.

While teleoperated platforms reduce radiation exposure and physical strain, they introduce new cognitive demands related to multi-degree-of-freedom controls and indirect haptic feedback[151]. Emerging interfaces that combine force-sensing catheters with high-fidelity haptic displays or augmented reality overlays are helping to shorten the learning curve[124]. Nevertheless, standardized metrics for performance assessment and credentialing remain lacking[152,153].

Cloud-connected robotic systems and remote tele-intervention have the potential to extend expert care beyond major medical centers[154,155]. At the same time, they raise critical issues around network reliability, cybersecurity, and equitable reimbursement models. Environmental impacts must also be considered, as miniaturized electronics and rare-earth magnets entail material costs that should be weighed against the potential benefits of reduced complications and shorter hospital stays.

Ultimately, addressing these challenges will require close, interdisciplinary collaboration among experts in materials

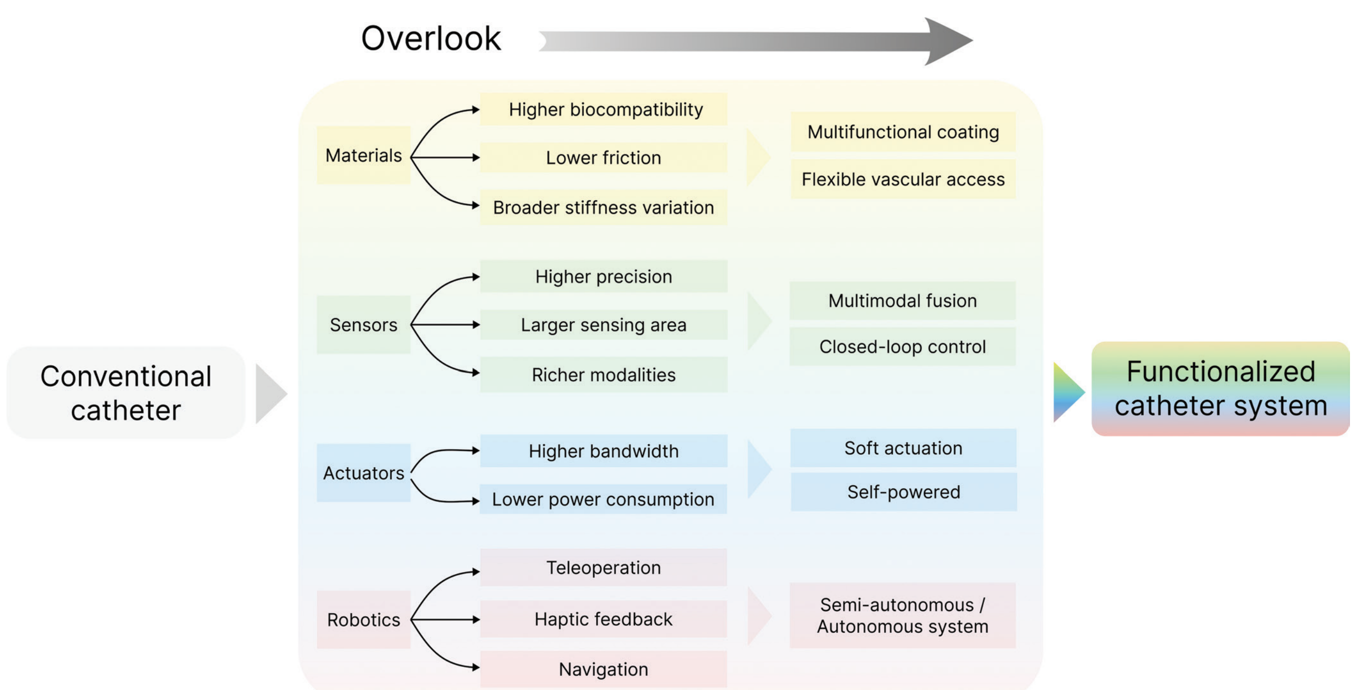

Figure 13. Future roadmap of functionalized catheter systems.

Table 1

Quantitative comparison between representative commercial and emerging endovascular systems.

Category	Subcategory	Commercial system and emerging system	Stiffness	Resolution	Speed	Size/compatibility	Comparative advantages of emerging systems
Material	Variable stiffness	Conventional gradient catheter (PTFE/PU composite)	Passive thermoplastic; 2–5× stiffness variation	–	–	Ø1–8 Fr; Length 100–150 cm	~10× higher stiffness tunability; faster response; improved thermal safety
		Piskarev et al.[49]	Actively tunable; 66× stiffness change	–	Hardening 4.4 s; Cooling <15 s	Ø2.3 mm; 20–37 °C; MR-compatible	
Sensor	IVUS imaging	Philips Eagle Eye Platinum	–	150 μm; Depth 8–10 mm	Rotation 100–1000 rps	Ø3.1–3.5 Fr	~3× higher resolution; NURD greatly reduced
		Han et al.[55]	–	51 μm; Depth 8 mm	12 fps	Transducer 0.55 × 0.45 mm²; PZT 30 μm	
	OCT imaging	Abbott Ilumien Optis	–	Axial 10–15 μm	180 fps	Ø2.7 Fr; minor distortion	2–5× faster scanning; smaller size; stable imaging
		Wang et al.[60]	–	Axial 5–10 μm	Rotation 10,000 rpm	Ø0.85 mm; distortion-free	
	FBG force sensing	Commercial RF ablation catheter	–	Force res. 5–10 mN; single axes	–	Ø1–2 mm; basic temp comp.	5–10× higher force resolution; multiaxis detection; temperature decoupling
		Li et al.[62,76]; Wang et al.[63]	–	0.52–0.64 mN (lateral); 23 mN (axial)	–	25–50 °C temp comp.; MRI-compatible	
Actuation	Ablation/mechanical cutting	Boston Scientific Rotablator	Variable, pneumatic	–	Rotation 190,000 rpm	Ø1.25–2.5 mm; Length 135 cm	Lower speed but stable torque; reduced friction and heat
		Heunis et al.[85]	Variable, magnetic drive	–	Torque 5.69 mN·m; Axial force 2.63 N	Ø3–4 mm; interchangeable tips	
	Steerable catheter	SwiftNINJA microcatheter	Fixed, pull-wire	–	Manual deflection 1–5 s	Ø2.9–2.4 Fr; Length 125–150 cm	~5× faster response; continuous curvature control
		Gopesh et al.[101]	Variable, hydraulic drive	–	Response <1 s; continuous 3D bending	Outer diameter <1 mm	
Robotics	Magnetic control	Stereotaxis Niobe	Fixed	Positioning accuracy <1 mm	Field response 1–2 s	–	Contact-free navigation; lower friction; better maneuverability
		Kim et al.[16]	Variable, magnetic drive	–	Navigation 5–10 mm/s; omnidirectional bending	MRI-compatible	
	Teleoperation/Haptics	CorPath GRX	–	Motion res. 0.1 mm	Bandwidth 5 Hz	Joystick interface for PCI	Improved haptic fidelity; enhanced safety and natural interaction
		Bao et al.[122]	–	Force res. 0.06 N; Torque res. 0.07 mN·m	Bandwidth 5 Hz; Latency <100 ms	Dual-hand control	

1 Fr, 0.33 m; Ø, outer diameter; rpm, rotations per minute; rps, rotations per second.

science, microfabrication, control engineering, and clinical medicine. The development of open hardware standards, accessible validation platforms (eg, ex vivo phantoms and animal models), and procedure-specific registries will be essential to accelerating the transition from laboratory research to clinical practice. In parallel, a phased approach to early stage human trials will be crucial for building the evidence base needed to ensure the safe, effective, and equitable deployment of next-generation intelligent catheter technologies.

8. Conclusion

This review provides a comprehensive overview of recent advances in intravascular catheters, including developments in materials, sensors, applications, and robotic integration. Intravascular catheters are shifting toward integrated, cyber-physical systems combining advanced materials, embedded sensing, and robotic control. While recent advances have enabled real-time navigation, force feedback, and adaptive mechanics, challenges remain in system-level integration, data fusion, and clinical validation. Future progress depends on developing compact, multifunctional architectures, standardized hardware platforms, and robust regulatory pathways. If these are addressed, next-generation catheters could offer autonomous navigation, intelligent compliance control, and precise therapy delivery, ushering in a new era of reproducible, data-driven endovascular interventions.

Funding

This work was supported by the National Key R&D Program of China grant (2024YFB3816000), Guangdong Innovative and Entrepreneurial Research Team Program

(2021ZT09L197), and Shenzhen Science and Technology Program (KJZD20240903100905008).

Conflicts of interests

The authors declare that they have no conflicts of interest.

Author contributions

Chuqiao Lyu and Wenbo Ding conceived the study. Chuqiao Lyu and Qinghao Xu conducted the literature search, and Chuqiao Lyu prepared the figures. Data curation and analysis were performed by Qinghao Xu, Eric J. Chen, and Wenxuan Zhu. The original draft of the manuscript was written by Chuqiao Lyu and Qinghao Xu. Shoujie Li, Hongliang Ren, and Wenbo Ding contributed to the review and editing of the manuscript. Wenbo Ding supervised the work and provided the funding. All authors read and approved the final manuscript.

References

[1] Ding R, Ren X, Sun Q, et al. Air pollution and stroke: an emerging challenge from cardio-cerebrovascular multimorbidity. *J Am Heart Assoc*. 2025;14(13):e041848.
[2] Li C, Bai C, Wang L, et al. Association between healthy lifestyle and cognitive decline, all-cause mortality, and mortality from cardiovascular and cerebrovascular diseases: a 10-year population-based prospective cohort study. *Alzheimers Dement*. 2025;21(3):e70021.
[3] Di Biase L, Lakkireddy DJ, Marazzato J, et al; ACC Electrophysiology and Interventional Councils. Antithrombotic therapy for patients undergoing cardiac electrophysiological and interventional procedures: JACC State-of-the-Art Review. *J Am Coll Cardiol*. 2024;83(1):82–108.
[4] Zhang M, Yang L, Yang H, et al. A magnetically actuated microcatheter with soft rotatable tip for enhanced endovascular access and treatment efficiency. *Sci Adv*. 2025;11(25):eadv1682.
[5] Peng Y, Liu X, Chan KF, et al. Robotic-assisted endovascular embolization: progress and future perspectives. *SmartBot*. 2025;1(1):e12009.
[6] Ren B, Zhao Y, Zhang J, et al. The critical technologies of vascular interventional robotic catheterization: a review. *IEEE Sens J*. 2023;23(24):30051–30069.
[7] Stone GW, Christiansen EH, Ali ZA, et al. Intravascular imaging-guided coronary drug-eluting stent implantation: an updated network meta-analysis. *Lancet (London, England)*. 2024;403(10429):824–837.
[8] Zhang P, Gao Y, Li S, et al. Waterborne polyurethane-stabilized hydrogel coating with lubrication and antibacterial properties on medical catheters. *ACS Appl Mater Interfaces*. 2025;17(16):24412–24420.
[9] Yang Z, Liu L, Li X, et al. Development and control of a dual-mode magnetic intravascular ultrasound robot for imaging in tortuous blood vessels. *IEEE/ASME Trans Mechatron*. 2025;30(1):168–179.
[10] Kundrat D, Dagnino G, Kwok TMY, et al. An MR-safe endovascular robotic platform: design, control, and ex-vivo evaluation. *IEEE Trans Biomed Eng*. 2021;68(10):3110–3121.
[11] Mei Z, Wei J, Pan S, et al. Transferring virtual surgical skills to reality: AI agents mastering surgical decision-making in vascular interventional robotics. *IEEE/ASME Trans Mechatron*. 2025;30(2):1261–1272.
[12] Rivkin B, Becker C, Singh B, et al. Electronically integrated microcatheters based on self-assembling polymer films. *Sci Adv*. 2021;7:eabl5408.
[13] Zhou C, Xu Z, Lin Z, et al. Submillimeter fiber robots capable of decoupled macro-micro motion for endoluminal manipulation. *Sci Adv*. 2024;10(47):eadr6428.
[14] Han M, Chen L, Aras K, et al. Catheter-integrated soft multilayer electronic arrays for multiplexed sensing and actuation during cardiac surgery. *Nat Biomed Eng*. 2020;4(10):997–1009.
[15] Lussi J, Mattmann M, Sevim S, et al. A submillimeter continuous variable stiffness catheter for compliance control. *Adv Sci*. 2021;8(18):e2101290.
[16] Kim Y, Parada GA, Liu S, et al. Ferromagnetic soft continuum robots. *Sci Robot*. 2019;4(33):eaax7329.
[17] Liu L, Yu H, Wang L, et al. Heparin-network-mediated long-lasting coatings on intravascular catheters for adaptive antithrombosis and antibacterial infection. *Nat Commun*. 2024;15(1):107.
[18] Chen Y, Yin R, Hong G. An "all-in-one" catheter: surgery of the future. *Matter*. 2020;3(6):1829–1831.
[19] Park J, Seo B, Jeong Y, et al. A review of recent advancements in sensor-integrated medical tools. *Adv Sci*. 2024;11(20):e2307427.
[20] Huang S, Huang X, Liu Z, et al. Advances in multifunctional electronic catheters for precise and intelligent diagnosis and therapy in minimally invasive surgery. *ACS Nano*. 2024;18(28):18129–18150.
[21] Veletić M, Apu EH, Simić M, et al. Implants with sensing capabilities. *Chem Rev*. 2022;122(21):16329–16363.
[22] Ogawa T, Sakakura K, Sumitsuji S, et al. Clinical expert consensus document on bailout algorithms for complications in percutaneous coronary intervention from the Japanese Association of Cardiovascular Intervention and Therapeutics. *Cardiovasc Interv Ther*. 2025;40(1):1–32.
[23] Agostoni P, Biondi-Zoccai G, De Benedictis M, et al. Radial versus femoral approach for percutaneous coronary diagnostic and interventional procedures-systematic overview and meta-analysis of randomized trials. *J Am Coll Cardiol*. 2004;44(2):349–356.
[24] Lydiard PGDip S, Blanck O, Hugo G, et al. A review of cardiac radioablation (CR) for arrhythmias: procedures, technology, and future opportunities. *Int J Radiat Oncol Biol Phys*. 2021;109(3):783–800.
[25] Staessens S, François O, Brinjikji W, et al. Studying stroke thrombus composition after thrombectomy: what can we learn? *Stroke*. 2021;52(11):3718–3727.
[26] Leyon JJ, Littlehales T, Rangarajan B, et al. Endovascular embolization: review of currently available embolization agents. *Curr Probl Diagn Radiol*. 2014;43(1):35–53.
[27] Angelini A, Barbera MD, Thiene G. Interventional procedures for atherothrombosis: pathology of retrieved material. *Heart*. 2007;93(10):1301–1308.
[28] Schatz RA. A view of vascular stents. *Circulation*. 1989;79(2):445–457.
[29] Goldmann DA, Pier GB. Pathogenesis of infections related to intravascular catheterization. *Clin Microbiol Rev*. 1993;6(2):176–192.
[30] Jalandhra GK, Srethbhakdi L, Davies J, et al. Materials advances in devices for heart disease interventions. *Adv Mater*. 2025;37(27):e2420114.
[31] Zhang X, Wang M, Liu L, et al. Hydrophobic-modified heparin coatings with adaptively anti-thrombotic and anti-bacterial functions for interventional cardiovascular catheters. *Chem Eng J*. 2025;514:163278.
[32] Wang B, Chan KF, Yuan K, et al. Endoscopy-assisted magnetic navigation of biohybrid soft microrobots with rapid endoluminal delivery and imaging. *Sci Robot*. 2021;6(52):eabd2813.
[33] Park S, Shin J, Jung J, et al. Polysaccharide-derivative coated intravascular catheters with superior multifunctional performance via simple and biocompatible method. *Chem Eng J*. 2022;433:134565.
[34] Zhang W, Du J, Kanwal F, et al. Study on PTFE superhydrophobic coating modified by IC@dMSNs and its enhanced antibacterial effect. *J Adv Res*. 2025;70:63–77.
[35] Radke D, Jia W, Sharma D, et al. Tissue engineering at the blood-contacting surface: a review of challenges and strategies in vascular graft development. *Adv Healthc Mater*. 2018;7(15):1701461.
[36] Wan X, Liu M, Zhang F, et al. Interfacial chemistry in functional hydrogel coatings. *Angew Chem Int Ed*. 2025;64(24):e202425552.
[37] Wang B, Shen J, Huang C, et al. Magnetically driven biohybrid blood hydrogel fibres for personalized intracranial tumour therapy under fluoroscopic tracking. *Nat Biomed Eng*. 2025;9:1471–1485.
[38] Coakley E, De Alba Nunez L, Honetschlager A, et al. Power of parametric: methods to validate ethylene oxide sterilization parametric release. *Biomed Instrum Technol*. 2023;57(4):129–135.
[39] Zbyrad B, Zaborniak M, Kochmański L, et al. Evaluation of high-temperature sterilization processes: their influence on the mechanical integrity of additively manufactured polymeric biomaterials. *Materials (Basel, Switzerland)*. 2025;18(6):1356.
[40] Lai C, Wang S, Zhong P, et al. A low-friction and high-stability hydrophilic PVP/PEG coated TPU for interventional catheter applications. *Tribol Int*. 2024;198:109859.
[41] Wang C, Hou Y, Wang X, et al. Structural and interfacial effects on drug release kinetics of liquid-based fibrous catheter. *Adv Fiber Mater*. 2022;4(6):1645–1655.
[42] Armugam A, Teong SP, Lim DSW, et al. Broad spectrum antimicrobial PDMS-based biomaterial for catheter fabrication. *Biomater Res*. 2021;25(1):33.
[43] Lim K, Chua R, Ho B, et al. Development of a catheter functionalized by a polydopamine peptide coating with antimicrobial and antibiofilm properties. *Acta Biomater*. 2015;15:127–138.
[44] Mattmann M, De Marco C, Briatico F, et al. Thermoset shape memory polymer variable stiffness 4D robotic catheters. *Adv Sci*. 2022;9(1):e2103277.
[45] Piskarev Y, Shintake J, Chautems C, et al. A variable stiffness magnetic catheter made of a conductive phase-change polymer for minimally invasive surgery. *Adv Funct Mater*. 2022;32(20):2107662.

[46] Mao L, Yang P, Tian C, et al. Magnetic steering continuum robot for transluminal procedures with programmable shape and functionalities. *Nat Commun*. 2024;15(1):3759.
[47] Sun Y, Piskarev Y, Hofstetter EH, et al. Instant variable stiffness in cardiovascular catheters based on fiber jamming. *Sci Adv*. 2025;11(6):eadn1207.
[48] Abdelaziz MEMK, Zhao J, Gil Rosa B, et al. Fiberbots: robotic fibers for high-precision minimally invasive surgery. *Sci Adv*. 2024;10(3):eadj1984.
[49] Piskarev Y, Sun Y, Righi M, et al. Fast-response variable-stiffness magnetic catheters for minimally invasive surgery. *Adv Sci*. 2024;11(12):e2305537.
[50] Choi J, Zheng Q, Abdelaziz MEMK, et al. Thermally drawn shape and stiffness programmable fibers for medical devices. *Adv Healthc Mater*. 2025;14(10):e2403235.
[51] Sung JH, Chang JH. Mechanically rotating intravascular ultrasound (IVUS) transducer: a review. *Sensors (Basel, Switzerland)*. 2021;21(11):3907.
[52] Magalhaes MA, Lipinski MJ, Minha S, et al. Aortic valve ChromaFlo®: a feasibility study of aortic regurgitation and effective annular aortic area assessment in a porcine model. *Cardiovasc Revasc Med*. 2014;15(3):156–159.
[53] Lee HF. TCTAP C-068 real-time intravascular ultrasound-guided recanalization of stumpless chronic total occlusion on both sides using a 7 Fr catheter via transradial approach. *JACC*. 2018;71(16):S136–S137.
[54] Pu Y, Li G, Zhang T, et al. Intravascular ultrasound imaging of pulmonary artery with high-altitude pulmonary hypertension. *Quant Imaging Med Surg*. 2024;14(4):3204–3209.
[55] Xu J, Wang N, Chu T, et al. A high-frequency mechanical scanning ultrasound imaging system. *Biosensors*. 2023;13(1):32.
[56] Hou S, Li Y, Zou C, et al. A novel distal micromotor-based side-looking intravascular ultrasound transducer. *IEEE Trans Ultrason Ferroelectr Freq Control*. 2022;69(1):283–290.
[57] Peng J, Ma L, Li X, et al. A novel synchronous micro motor for intravascular ultrasound imaging. *IEEE Trans Biomed Eng*. 2019;66(3):802–809.
[58] Han Z, Wang N, Zhu X, et al. A miniature high-frequency rotary ultrasonic encoder for internal ultrasound imaging. *IEEE Sens J*. 2021;21(12):13137–13145.
[59] Liu B, Su M, Zhang Z, et al. A novel dual-element catheter for improving non-uniform rotational distortion in intravascular ultrasound. *IEEE Trans Biomed Eng*. 2023;70(6):1768–1774.
[60] Wang B, Tao K, Hu X, et al. Intravascular optical coherence tomography utilizing a miniature piezoelectric-driven probe. *IEEE Trans Biomed Eng*. 2023;70(12):3490–3500.
[61] Yuan W, Chen D, Sarabia-Estrada R, et al. Theranostic OCT microneedle for fast ultrahigh-resolution deep-brain imaging and efficient laser ablation in vivo. *Sci Adv*. 2020;6(15):eaaz9664.
[62] Li T, Pan A, Ren H. A high-resolution triaxial catheter tip force sensor with miniature flexure and suspended optical fibers. *IEEE Trans Ind Electron*. 2020;67(6):5101–5111.
[63] Wang Z, Qiu Y, Chen J, et al. A novel FBG-based tri-axis tip force sensor: design, modeling, and application. *IEEE/ASME Trans Mechatron*. 2025:1–12.
[64] Dong Z, Wang X, Fang G, et al. Shape tracking and feedback control of cardiac catheter using MRI-guided robotic platform—validation with pulmonary vein isolation simulator in MRI. *IEEE Trans Robot*. 2022;38(5):2781–2798.
[65] Zhang T, Li G, Ren H, et al. Sub-millimeter fiberscopic robot with integrated maneuvering, imaging, and biomedical operation abilities. *Nat Commun*. 2024;15(1):10874.
[66] Araki M, Park SJ, Dauerman HL, et al. Optical coherence tomography in coronary atherosclerosis assessment and intervention. *Nat Rev Cardiol*. 2022;19(10):684–703.
[67] Tearney GJ, Brezinski ME, Bouma BE, et al. In vivo endoscopic optical biopsy with optical coherence tomography. *Science*. 1997;276(5321):2037–2039.
[68] Tsai TH, Adler D. ILUMIEN OPTIS Mobile and OPTIS Integrated Technology Overview. In: *OCT Made Easy*. CRC Press; 2017.
[69] Yuan W, Brown R, Mitzner W, et al. Super-achromatic monolithic microprobe for ultrahigh-resolution endoscopic optical coherence tomography at 800 nm. *Nat Commun*. 2017;8(1):1531.
[70] Li J, Thiele S, Quirk BC, et al. Ultrathin monolithic 3D printed optical coherence tomography endoscopy for preclinical and clinical use. *Light Sci Appl*. 2020;9(1):124.
[71] Pahlevaninezhad H, Khorasaninejad M, Huang YW, et al. Nano-optic endoscope for high-resolution optical coherence tomography in vivo. *Nat Photonics*. 2018;12(9):540–547.
[72] Zhang T, Yuan S, Xu C, et al. PneumaOCT: pneumatic optical coherence tomography endoscopy for targeted distortion-free imaging in tortuous and narrow internal lumens. *Sci Adv*. 2024;10(35):eadp3145.
[73] Yuan S, Xu C, Cui B, et al. Motor-free telerobotic endomicroscopy for steerable and programmable imaging in complex curved and localized areas. *Nat Commun*. 2024;15(1):7680.
[74] Abouraddy AF, Bayindir M, Benoit G, et al. Towards multimaterial multifunctional fibres that see, hear, sense and communicate. *Nat Mater*. 2007;6(5):336–347.
[75] Akinyemi TO, Omisore OM, Duan W, et al. Fiber Bragg grating-based force sensing in robot-assisted cardiac interventions: a review. *IEEE Sens J*. 2021;21(9):10317–10331.
[76] Li T, Shi C, Ren H. Three-dimensional catheter distal force sensing for cardiac ablation based on fiber Bragg grating. *IEEE/ASME Trans Mechatron*. 2018;23(5):2316–2327.
[77] Kwon K, Kim JU, Won SM, et al. A battery-less wireless implant for the continuous monitoring of vascular pressure, flow rate and temperature. *Nat Biomed Eng*. 2023;7(10):1215–1228.
[78] Shen X, Jia E, Huang Y, et al. Bioinspired balloon catheter integrated with stretchable "flounder" electrodes under high voltage for uniform pulsed field ablation. *Sci Adv*. 2024;10(50):eadq5822.
[79] Xue J, Qin C, Cai D, et al. Scalable balloon catheter assisted contact enhancement of 3D electrode array for colon electrophysiological recording. *Sens Actuators B*. 2025;424:136955.
[80] Lee SP, Klinker LE, Ptaszek L, et al. Catheter-based systems with integrated stretchable sensors and conductors in cardiac electrophysiology. *Proc IEEE*. 2015;103(4):682–689.
[81] Singh M, Varela CE, Whyte W, et al. Minimally invasive electroceutical catheter for endoluminal defect sealing. *Sci Adv*. 2021;7(14):eabf6855.
[82] Cheng T, Shao J, Wang ZL. Triboelectric nanogenerators. *Nat Rev Methods Primer*. 2023;3(1):1–13.
[83] Nguyen TK, Yadav S, Truong TA, et al. Integrated, transparent silicon carbide electronics and sensors for radio frequency biomedical therapy. *ACS Nano*. 2022;16(7):10890–10903.
[84] Xu M, Song Z, Hong W, et al. A high-precision, low-voltage pulsed field ablation device with capability of minimally invasive surgery. *Adv Funct Mater*. 2023;33(38):2302041.
[85] Heunis CM, Behrendt KJ, Hekman EEG, et al. Design and evaluation of a magnetic rotablation catheter for arterial stenosis. *IEEE/ASME Trans Mechatron*. 2022;27(3):1761–1772.
[86] Yang Z, Yang L, Zhang M, et al. Ultrasound-guided catheterization using a driller-tipped guidewire with combined magnetic navigation and drilling motion. *IEEE/ASME Trans Mechatron*. 2022;27(5):2829–2840.
[87] Huang S, He M, Yao C, et al. Petromyzontidae-biomimetic multimodal microneedles-integrated bioelectronic catheters for theranostic endoscopic surgery. *Adv Funct Mater*. 2023;33(15):2214485.
[88] Xu M, Song Z, Peng Q, et al. Catheter-integrated fractal microelectronics for low-voltage ablation and minimally invasive sensing. *ACS Sens*. 2025;10(4):2779–2789.
[89] Starek Z, Soucek F, Dolezalova K, et al. A prospective randomized clinical comparison of catheter ablation of atrial fibrillation using the CENTAURI PEF system and standard radiofrequency ablation. *Europace*. 2025;27(Suppl_1):euaf085–euaf184.
[90] Tanese N, Almorad A, Pannone L, et al. Outcomes after cryoballoon ablation of paroxysmal atrial fibrillation with the PolarX or the Arctic Front Advance Pro: a prospective multicentre experience. *Europace*. 2023;25(3):873–879.
[91] Guo M, Qu L, Zhang N, et al. Comparison of the lesion formation and safety in ex vivo porcine heart study: using Thermocool SmartTouch and Thermocool SmartTouch-SF catheters. *J Cardiovasc Electrophysiol*. 2021;32(8):2077–2089.
[92] Koh A, Gutbrod SR, Meyers JD, et al. Ultrathin injectable sensors of temperature, thermal conductivity, and heat capacity for cardiac ablation monitoring. *Adv Healthc Mater*. 2016;5(3):373–381.
[93] Khattak S, Sharma H, Khan SQ. Atherectomy techniques: rotablation, orbital and laser. *Interv Cardiol*. 2024;19:e21.
[94] Yinadsawaphan T, Kulthamrongsri N, Baquero G. Abstract 4142716: double guiding catheter technique for orbital atherectomy in a heavily calcified coronary bifurcation using microcatheter protection for non-atherectomy wire. *Circulation*. 2024;150(Suppl_1):A4142716–A4142716.
[95] Khalil ISM, Tabak AF, Sadek K, et al. Rubbing against blood clots using helical robots: modeling and in vitro experimental validation. *IEEE Robot Autom Lett*. 2017;2(2):927–934.
[96] Girerd C, Morimoto TK. Design and control of a hand-held concentric tube robot for minimally invasive surgery. *IEEE Trans Robot*. 2021;37(4):1022–1038.

[97] Rogatinsky J, Recco D, Feichtmeier J, et al. A multifunctional soft robot for cardiac interventions. *Sci Adv*. 2023;9(43):eadi5559.
[98] Nguyen CC, Hoang TT, Davies J, et al. Soft fibrous syringe architecture for electricity-free and motorless control of flexible robotic systems. *Adv Sci*. 2024;11(39):e2405610.
[99] Ali A, Plettenburg DH, Breedveld P. Steerable catheters in cardiology: classifying steerability and assessing future challenges. *IEEE Trans Biomed Eng*. 2016;63(4):679–693.
[100] Da Veiga T, Chandler JH, Lloyd P, et al. Challenges of continuum robots in clinical context: a review. *Prog Biomed Eng*. 2020;2(3):032003.
[101] Gopesh T, Wen JH, Santiago-Dieppa D, et al. Soft robotic steerable microcatheter for the endovascular treatment of cerebral disorders. *Sci Robot*. 2021;6(57):eabf0601.
[102] Kim MS, Park CY, Lee DY. Magnetorheological-elastomer-based and hydraulically steerable actuator for micro guidewire and catheter. *IEEE Trans Med Robot Bionics*. 2025;7(1):77–84.
[103] Ding D, Yao T, Wang H, et al. Continuum robotic catheter systems for transcatheter mitral valve procedures: a technical review. *IEEE Access*. 2025;13:43275–43288.
[104] Dupont PE, Simaan N, Choset H, et al. Continuum robots for medical interventions. *Proc IEEE Inst Electr Electron Eng*. 2022;110(7):847–870.
[105] Bonatti J, Vetrovec G, Riga C, et al. Robotic technology in cardiovascular medicine. *Nat Rev Cardiol*. 2014;11(5):266–275.
[106] Roshanfar M, Salimi M, Kaboodrangi AH, et al. Advanced robotics for the next-generation of cardiac interventions. *Micromachines*. 2025;16(4):363.
[107] Dreyfus R, Boehler Q, Lyttle S, et al. Dexterous helical magnetic robot for improved endovascular access. *Sci Robot*. 2024;9(87):eadh0298.
[108] Phelan MF III, Tiryaki ME, Lazovic J, et al. Heat-mitigated design and Lorentz force-based steering of an MRI-driven microcatheter toward minimally invasive surgery. *Adv Sci*. 2022;9(10):2105352.
[109] Tiryaki ME, Elmacıoğlu YG, Sitti M. Magnetic guidewire steering at ultrahigh magnetic fields. *Sci Adv*. 2023;9(17):eadg6438.
[110] Hwang J, Jeon S, Kim B, et al. An electromagnetically controllable microrobotic interventional system for targeted, real-time cardiovascular intervention. *Adv Healthc Mater*. 2022;11(11):e2102529.
[111] Pittiglio G, Leuenberger F, Mencattelli M, et al. Magnetic ball chain robots for cardiac arrhythmia treatment. *IEEE Trans Med Robot Bionics*. 2024;6(4):1322–1333.
[112] Kim Y, Zhao X. Magnetic soft materials and robots. *Chem Rev*. 2022;122(5):5317–5364.
[113] Yang Z, Yang H, Cao Y, et al. Magnetically actuated continuum medical robots: a review. *Adv Intell Syst*. 2023;5(6):2200416.
[114] Limpabandhu C, Hu Y, Ren H, et al. Actuation technologies for magnetically guided catheters. *Minim Invasive Ther Allied Technol*. 2023;32(4):137–152.
[115] Wang Q, Zhao F, Wang B, et al. Untethered miniature robots for minimally invasive thrombus treatment: from bench to clinical trials. *Innovation (Cambridge, Mass.)*. 2025;6(6):100874.
[116] Torlakcik H, Sevim S, Alves P, et al. Magnetically guided microcatheter for targeted injection of magnetic particle swarms. *Adv Sci*. 2024;11(38):e2404061.
[117] Yan Y, Wang T, Zhang R, et al. Magnetically assisted soft milli-tools for occluded lumen morphology detection. *Sci Adv*. 2023;9(33):eadi3979.
[118] Wang C, Wang T, Li M, et al. Heterogeneous multiple soft millirobots in three-dimensional lumens. *Sci Adv*. 2024;10(45):eadq1951.
[119] Jin X, Guo S, Guo J, et al. Development of a tactile sensing robot-assisted system for vascular interventional surgery. *IEEE Sens J*. 2021;21(10):12284–12294.
[120] Jin X, Guo S, Guo J, et al. Total force analysis and safety enhancing for operating both guidewire and catheter in endovascular surgery. *IEEE Sens J*. 2021;21(20):22499–22509.
[121] Jin X, Guo S, Song A, et al. A novel robotic platform for endovascular surgery: human–robot interaction studies. *IEEE Trans Instrum Meas*. 2024;73(4000509):1–9.
[122] Bao X, Guo S, Shi L, et al. Design and evaluation of sensorized robot for minimally vascular interventional surgery. *Microsyst Technol*. 2019;25(7):2759–2766.
[123] Bao X, Guo S, Yang C, et al. Haptic interface with force and torque feedback for robot-assisted endovascular catheterization. *IEEE/ASME Trans Mechatron*. 2024;29(2):1111–1125.
[124] Hooshiar A, Najarian S, Dargahi J. Haptic telerobotic cardiovascular intervention: a review of approaches, methods, and future perspectives. *IEEE Rev Biomed Eng*. 2020;13:32–50.
[125] Hooshiar A, Sayadi A, Dargahi J, et al. Integral-free spatial orientation estimation method and wearable rotation measurement device for robot-assisted catheter intervention. *IEEE/ASME Trans Mechatron*. 2021;27:766–776.
[126] Kim Y, Genevriere E, Harker P, et al. Telerobotic neurovascular interventions with magnetic manipulation. *Sci Robot*. 2022;7(65):eabg9907.
[127] Dagnino G, Kundrat D, Kwok TMY, et al. In-vivo validation of a novel robotic platform for endovascular intervention. *IEEE Trans Biomed Eng*. 2023;70(6):1786–1794.
[128] Mendes Pereira V, Rice H, De Villiers L, et al. Evaluation of effectiveness and safety of the CorPath GRX robotic system in endovascular embolization procedures of cerebral aneurysms. *J Neurointerv Surg*. 2024;16(4):405–411.
[129] Tomasello A, Hernández D, Li J, et al. Modeling robotic-assisted mechanical thrombectomy procedures with the CorPath GRX robot: the core-flow study. *AJNR Am J Neuroradiol*. 2024;45(6):721–726.
[130] Durand E, Sabatier R, Smits PC, et al. Evaluation of the R-one robotic system for percutaneous coronary intervention: the R-EVOLUTION study. *EuroIntervention*. 2023;18(16):e1339–e1347.
[131] Cao S, Guo S, Guo J, et al. A reciprocating delivery device-based endovascular intervention robot with multi-manipulators collaboration. *IEEE Trans Instrum Meas*. 2023;73(4001812):1–12.
[132] Šuligoj F, Heunis CM, Mohanty S, et al. Intravascular tracking of micro-agents using medical ultrasound: towards clinical applications. *IEEE Trans Biomed Eng*. 2022;69(12):3739–3747.
[133] Yang Z, Yang L, Zhang L. Autonomous navigation of magnetic microrobots in a large workspace using mobile-coil system. *IEEE/ASME Trans Mechatron*. 2021;26(6):3163–3174.
[134] Yang L, Jiang J, Gao X, et al. Autonomous environment-adaptive microrobot swarm navigation enabled by deep learning-based real-time distribution planning. *Nat Mach Intell*. 2022;4(5):480–493.
[135] Yang L, Jiang J, Ji F, et al. Machine learning for micro- and nanorobots. *Nat Mach Intell*. 2024;6(6):605–618.
[136] Wang Q, Chan KF, Schweizer K, et al. Ultrasound Doppler-guided real-time navigation of a magnetic microswarm for active endovascular delivery. *Sci Adv*. 2021;7(9):eabe5914.
[137] Ramadani A, Bui M, Wendler T, et al. A survey of catheter tracking concepts and methodologies. *Med Image Anal*. 2022;82:102584.
[138] Klein A, Guild J, Xi Y, et al. Use of a 2 dimensional vessel navigator roadmap decreases patient radiation dose compared to standard 3D mapping for fenestrated endovascular aneurysm repair. *Ann Vasc Surg*. 2022;80:250–255.
[139] Malafosse C, Massiot N, Guimo F, et al. Impact of the endonaut® angio-navigation system on radiation exposure in endovascular aortic repair performed with mobile C-arms. *Ann Vasc Surg*. 2024;109:143–148.
[140] Burnett E, Samburg B, Olmstead A, et al. IOPS-guided antegrade insitu laser fenestration in an aortic model. *J Vasc Surg*. 2025;81(5):S67–S68.
[141] Vandini A, Glocker B, Hamady M, et al. Robust guidewire tracking under large deformations combining segment-like features (SEGlets). *Med Image Anal*. 2017;38:150–164.
[142] Abdelaziz MEMK, Tian L, Hamady M, et al. X-ray to MR: the progress of flexible instruments for endovascular navigation. *Prog Biomed Eng*. 2021;3(3):032004.
[143] Kilbride BF, Narsinh KH, Jordan CD, et al. MRI-guided endovascular intervention: current methods and future potential. *Expert Rev Med Devices*. 2022;19(10):763–778.
[144] Azizi A, Tremblay CC, Gagné K, et al. Using the fringe field of a clinical MRI scanner enables robotic navigation of tethered instruments in deeper vascular regions. *Sci Robot*. 2019;4(36):eaax7342.
[145] Felfoul O, Becker A, Bergeles C, et al. Achieving commutation control of an MRI-powered robot actuator. *IEEE Trans Robot*. 2015;31(2):387–399.
[146] Fagogenis G, Mencattelli M, Machaidze Z, et al. Autonomous robotic intracardiac catheter navigation using haptic vision. *Sci Robot*. 2019;4(29):eaaw1977.
[147] Kim DH, Lu N, Ghaffari R, et al. Materials for multifunctional balloon catheters with capabilities in cardiac electrophysiological mapping and ablation therapy. *Nat Mater*. 2011;10(4):316–323.
[148] Deng J, Yuk H, Wu J, et al. Electrical bioadhesive interface for bioelectronics. *Nat Mater*. 2021;20(2):229–236.
[149] Shen Y, Wang Z, Wang Z, et al. Thermally drawn multifunctional fibers: toward the next generation of information technology. *InfoMat*. 2022;4(7):e12318.
[150] Yang H, Shan C, Kolen AF, et al. Medical instrument detection in ultrasound: a review. *Artif Intell Rev*. 2023;56(5):4363–4402.
[151] Yan Y, Wang H, Yu H, et al. Machine learning-based surgical state perception and collaborative control for a vascular interventional robot. *IEEE Sens J*. 2022;22(7):7106–7118.

[152] Zhou XH, Xie XL, Liu SQ, et al. Learning skill characteristics from manipulations. *IEEE Trans Neural Netw Learn Syst*. 2023;34(12):9727–9741.
[153] Zhou XH, Bian GB, Xie XL, et al. An interventionalist-behavior-based data fusion framework for guidewire tracking in percutaneous coronary intervention. *IEEE Trans Syst Man Cybern Syst*. 2020;50(11):4836–4849.
[154] Yang C, Guo S, Guo Y, et al. Cloud communication-based sensing performance evaluation of a vascular interventional robot system. *IEEE Sens J*. 2022;22(9):9005–9017.
[155] Mahmud E, Madder RD, Wohns DH, et al. Robotic-assisted percutaneous coronary intervention: final results of the PRECISION and PRECISION GRX studies. *J Soc Cardiovasc Angiogr Interv*. 2025;4(7):103655.

How to cite this article: Lyu C, Xu Q, Li S, Chen EJ, Zhu W, Ren H, Ding W. Functional advancements in intravascular catheters: materials, sensors, actuators, and robot integration. MedMat 2025;2(4):e00031. doi: 10.1097/mm9.0000000000000031